GALACTIC H II REGIONS. II. OBSERVATIONS OF THEIR HYDROGEN 109α RECOMBINATION-LINE RADIATION AT THE FREQUENCY 5009 MHz

P. G. MEZGER AND B. HÖGLUND*
National Radio Astronomy Observatory,† Green Bank, West Virginia
Received June 10, 1966; revised August 22, 1966

ABSTRACT

The hydrogen 109α recombination-line spectrum of twenty galactic radio sources has been investigated, using a 20-channel frequency switched line radiometer (channel width 95 kHz) together with the NRAO 140-foot telescope. Sixteen of the investigated sources show line emission. The observations yield the ratio of excess line to free-free continuum temperature $(T_{L+C} - T_C)/T_C$ and the radial velocity of the H II region. The line width $\Delta\nu_L$ was determined by fitting a Gaussian profile to the observed points.

The kinematic distances of the H II regions are estimated from the observed radial velocities. The distribution of the H II regions, projected on the galactic plane, is compared with a similar analysis from optically derived distances of H II regions in the vicinity of the Sun made by Becker and Fenkart. The rms velocity of the peculiar motion of the H II regions is found to be less than 7 km/sec.

The electron temperatures of the H II regions are determined from the observed quantity $\Delta\nu_L(T_{C+L} - T_C)/T_C$, assuming thermal equilibrium. A mean value of 5800° K is found with individual values ranging from 4000° to 9500° K. Our observational results are compared with Goldberg's prediction of enhanced line radiation due to stimulated emission.

Since Doppler broadening is the only effective broadening mechanism for the observed 109α lines, the rms velocity of the internal turbulence in the H II regions has been determined from the observed line widths. The mean value of fifteen H II regions yields 19.25 km/sec, a value which is more than twice the velocity of sound at $T_e = 5800°$ K.

The non-detection of the 109α line is used to identify non-thermal sources in the Sgr A region and in the radio source associations W49 and W51.

The velocity dispersion of H II regions and nearby OH clouds which show the 18-cm line in emission is found to be 7.9 km/sec.

I. INTRODUCTION

After the first detection of the hydrogen recombination line 109α with the rest frequency 5008.932 MHz on July 9 (Höglund and Mezger 1965), we started a search for this line in twenty galactic sources. This line survey yielded the following information: (i) whether the investigated radio sources were thermal or non-thermal (through the presence or absence of the line radiation); (ii) excess line temperature as compared to the free-free continuum temperature; (iii) half-power width (HPW); and (iv) shift of the center frequency with respect to the rest frequency of the hydrogen recombination line. This frequency shift $\Delta\nu$ is converted into a radial velocity using the relation

$$\left(\frac{v_r}{\text{km/sec}}\right) = -5.985 \times 10^{-2} \left(\frac{\Delta\nu}{\text{kHz}}\right). \quad (1)$$

A radial velocity of 1 km/sec causes a frequency shift of 16.71 kHz. A definite correlation is established between the radio radial velocities and the radial velocities derived from optical observations of the bright lines of the emission nebulae. Using galactic rotation parameters based on several models, we estimate (v) the distances of the observed H II regions and obtain their distribution in the galactic plane. These distances are compared with the photometric distances in those cases where the radio source is unambiguously identified with an optical emission nebula.

* Present address: Onsala Space Observatory, Chalmers Institute of Technology, Gothenburg, Sweden.

† The National Radio Astronomy Observatory is operated by Associated Universities, Inc., under contract with the National Science Foundation.

The survey of the continuum emission of the H II regions included in the line survey (Mezger and Henderson 1966; referred to hereinafter as "Paper I") provided us with the peak temperature T_c of the free-free emission. Combining this quantity with the observational results listed under (ii) and (iii), we derive in this paper (vi) the average electron temperature, and (vii) the rms velocity of the internal motion of the investigated H II regions.

II. OBSERVING INSTRUMENT, OBSERVING PROCEDURE, AND DATA REDUCTION

The observations were performed with a 20-channel receiver, the width of one channel being 95 kHz. This line receiver, its calibration, and the way the line observations were performed have been described in another paper (Höglund and Mezger 1965). The frequency stability of this line receiver is in the order of 10^{-8} per day. It was installed on the NRAO 140-foot telescope whose characteristics at $\lambda = 6$ cm are described in Paper I.

The results of the line survey are compiled in Table 1. The first column gives the optical or radio source designation under which the source is best known; the second column gives the number of the source in galactic coordinate notation. This new system of designating galactic sources is described in Paper I. The third column gives the center line temperature T_L with an accuracy of $_{-9}^{+36}$ per cent.[1] The fourth column gives the ratio of the center line temperature to the continuum temperature T_C of the source. The values T_C have been taken from Paper I, Table 3, column 14.[2] The accuracy of the communicated ratios T_L/T_C is $_{-9}^{+36}$ per cent.

The observed profiles are shown in Figure 1. Both frequency and radial velocity scales in this figure refer to the local standard of rest (LSR), assuming the standard solar motion of 20.0 km/sec toward $l^{II} = 56\overset{\circ}{.}2$ and $b^{II} = +22\overset{\circ}{.}8$. The full curves are Gaussian curves of best fit. The half-power width $\Delta\nu_L$ of the Gaussian curves, not corrected for the radiometer band pass, is given in the fifth column. The quoted errors are the standard deviations from the least-squares fit of the Gaussian curves. The sixth column gives the product of line width $\Delta\nu_L$ times the ratio T_L/T_C in kHz. Since the errors in the measurement of both quantities are uncorrelated, they have been added geometrically.

The deviation between the center frequency of the Gaussian line profiles of best fit and the rest frequency of the 109α line (reduced to the LSR), $\Delta\nu$, is given in the seventh column. The heliocentric radial velocities corresponding to the frequency shifts are given in the eighth column. For comparison purposes, the radial velocities of emission nebulae obtained from optical observations are given in the ninth column. The radio radial velocities, reduced to LSR, are given in the tenth column.

With both signal and comparison *LO*'s fixed, the total analyzing width of the 20-channel receiver is 2 MHz. During the various observations the signal *LO* was shifted occasionally in order to increase the effective frequency range of the observations. Hence, the outer points in the profiles have been observed with a shorter integration time, and their statistical weights are smaller than those of the central points.

III. DETERMINATION OF THE KINEMATIC DISTANCE

If we adopt a model of the galactic rotation, the observed radial velocities can be converted into distances. We used the Australian Conference Model (referred to in the fol-

[1] This error is nearly exclusively due to calibration errors of the line calibration mark. We obtained values of 6 4° K (June 16); 7 5° K (July 16); and 5 0° K (August 14). This range of values was due only to reading errors on the analogue records; it is not inherent in the calibration circuitry. The value 7.5° K was adopted for the reduction of our first line observations (Höglund and Mezger 1965). Considering the quality of the different calibrations, we obtain now a weighted mean value of $T(\mathrm{Cal}) = 5.5_{-0.5}^{+2\ 0}$ °K, which was used for the evaluation of the line observations in this paper

[2] Note that in our notation T_A (source) is the antenna temperature corrected for atmospheric extinction while T_C is the measured antenna temperature with no extinction correction. The excess line temperature, T_L, has no extinction correction and the ratio T_L/T_C is free of extinction effects if both are measured under the same conditions.

TABLE 1

RESULTS OF A SURVEY OF THE HYDROGEN 109α LINE IN GALACTIC RADIO SOURCES

NAME OF SOURCE	RADIO COMPONENT	T_L (° K)	T_L/T_C (Per Cent)	$\Delta\nu_L$ (kHz)	$\Delta\nu_L T_L/T_C$ (kHz)	$\Delta\nu$ (kHz)	v_r (heliocentric)(km/sec)			v_r(LSR) (km/sec)	REMARKS
							Radio	Optical		Radio	
								(1)*	(2)*		
IC 1795.....	G133.7+1.2	0.79	5.5	594 (±11%)	$32.7\,(^{+38\%}_{-14\%})$	+726±50	−47.7±3.0	−48.0	.....	−43.5±3.0	Optical radial velocity has been measured for IC 1805 only
	G133.8+1.4	0.22	4.1	395 (±10%)	$16.1\,(^{+37\%}_{-13\%})$	+842±21	−54.6±1.3	.....	.....	−50.4±1.3	
Orion A.....	G209.0−19.4	3.52	5.2	485 (± 4%)	$25.2\,(^{+36\%}_{-10\%})$	+ 34±20	+16.1±1.2	+18.0	+17.5	− 2.0±1.2	T_L(He)/T_L(H)<0.05 rms
	3′ north	2.47	6.3	460 (±10%)	$29.2\,(^{+37\%}_{-13\%})$	+ 44±40	+15.1±2.4	.....	.....	− 2.6±2.4	
	3′ south	3.28	5.7	607 (± 7%)	$34.4\,(^{+37\%}_{-11\%})$	+117±42	+11.1±2.5	.....	.....	− 7.0±2.5	
	12^s west	2.61	6.7	782 (± 8%)	$52.3\,(^{+37\%}_{-12\%})$	+158±52	+ 8.6±3.1	.....	.....	− 9.5±3.1	
	12^s east	2.95	5.2	478 (±16%)	$24.7\,(^{+39\%}_{-18\%})$	+ 40±40	+15.7±2.4	.....	.....	− 2.4±2.4	
IC 434.....	G206.5−16.4	0.78	6.6	374 (± 6%)	$24.7\,(^{+36\%}_{-11\%})$	− 74±20	+21.9±1.2	+37.0	.....	+ 4.4±1.2	Campbell and Paddock were unable to detect bright lines (3)*
NGC 6357...	G353.2+0.9	0.97	6.1	450 (± 6%)	$27.4\,(^{+36\%}_{-11\%})$	+ 20±23	− 9.7±1.4	.....	.....	− 1.2±1.4	
	G353.2+0.7	0.85	5.7	527 (±12%)	$29.9\,(^{+38\%}_{-15\%})$	− 98±40	−14.4±2.4	.....	.....	− 5.9±2.4	
Sgr A.....	G0.0−0.0	<0.23 rms	<0.62 rms	.....	.....	.....	.....	.....	.....	.....	Spectrum analyzed: $-87 \le v_r(\mathrm{LSR}) \le +99$ km/sec
		<0.39 rms	<1.06 rms	.....	.....	.....	.....	.....	.....	.....	$-87 \le v_r(\mathrm{LSR}) \le +141$ km/sec
	G0.2−0.1	0.47	4.3	572 (±11%)	$24.9\,(^{+38\%}_{-14\%})$	−992±50	+49.1±3.0	.....	.....	+59.4±3.0	
	G0.6−0.1	<0.18 rms	<2.1 rms	.....	.....	.....	.....	.....	.....	.....	$-50 \le v_r(\mathrm{LSR}) \le +70$ km/sec
	G0.7−0.1	0.43	3.6	817 (±13%)	$29.7\,(^{+38\%}_{-16\%})$	+415±75	−35.2±4.5	.....	.....	−24.9±4.5	
M8.....	G6.0−1.2	0.68	7.0	403 (±12%)	$28.3\,(^{+38\%}_{-15\%})$	− 58±32	− 8.1±1.9	− 7.1	− 3.0	+ 3.5±1.9	
W31.....	G10.3−0.2	0.63	5.1	563 (± 8%)	$28.6\,(^{+37\%}_{-12\%})$	−181±32	− 1.9±1.9	.....	.....	+10.8±1.9	
M16.....	G16.9+0.8	0.37	7.4	365 (±16%)	$27.2\,(^{+39\%}_{-18\%})$	−466±60	+13.5±3.6	.....	.....	+27.9±3.6	

* References: (1) Courtès (1960); (2) Campbell and Moore, as quoted by Wilson (1953); (3) Campbell and Moore (1918).

TABLE 1—*Continued*

Name of Source	Radio Component	T_L (° K)	T_L/T_C (Per Cent)	$\Delta\nu_L$ (kHz)	$\Delta\nu_L T_L/T_C$ (kHz)	$\Delta\nu$ (kHz)	v_r (heliocentric) (km/sec)			v_r(LSR) (km/sec)	Remarks
							Radio	Optical (1)*	Optical (2)*	Radio	
M17	G15.0−0.7	3.88	5.3	643 (± 4%)	$34.1\left(^{+36\%}_{-10\%}\right)$	− 294±30	+ 3.8±1.8		+ 7.2	+17.6±1.8	T_L(He)/T_L(H) <0.12 rms
	3′ north	2.82	4.8	645 (±10%)	$31.1\left(^{+37\%}_{-13\%}\right)$	− 222±40	− 0.5±2.4			+13.3±2.4	
	3′ south	3.33	6.5	507 (± 5%)	$33.0\left(^{+36\%}_{-11\%}\right)$	− 281±21	+ 3.0±1.3			+16.8±1.3	
	12^s.5 west	2.56	5.9	587 (± 5%)	$34.8\left(^{+36\%}_{-11\%}\right)$	− 272±24	+ 2.5±1.4			+16.3±1.4	
	12^s.5 east	3.22	6.1	545 (± 5%)	$33.2\left(^{+36\%}_{-11\%}\right)$	− 293±25	+ 3.7±1.4			+17.5±1.4	
W43	G30.8−0.0	1.01	6.3	697 (± 7%)	$43.7\left(^{+37\%}_{-11\%}\right)$	−1479±30	+71.9±1.8			+88.6±1.8	
W49	G43.2+0.0	0.73	5.8	445 (± 8%)	$25.6\left(^{+37\%}_{-12\%}\right)$	− 123±34	−10.6±2.0			+ 7.4±2.0	
	G43.3−0.2	<0.08 rms	<1.9 rms								
W51	G49.0−0.3	0.30	4.7	345 (±13%)	$16.1\left(^{+38\%}_{-16\%}\right)$	−1076±50	+48.2±3.0			+66.4±3.0	
	G49.5−0.4	1.36	6.3	695 (± 6%)	$43.5\left(^{+36\%}_{-11\%}\right)$	− 987±35	+40.9±2.1			+59.1±2.1	
W75	G81.7+0.5	<0.13 rms	<2.1 rms								Spectrum analyzed: $-108 \leq v_r(\mathrm{LSR}) \leq +186$ km/sec

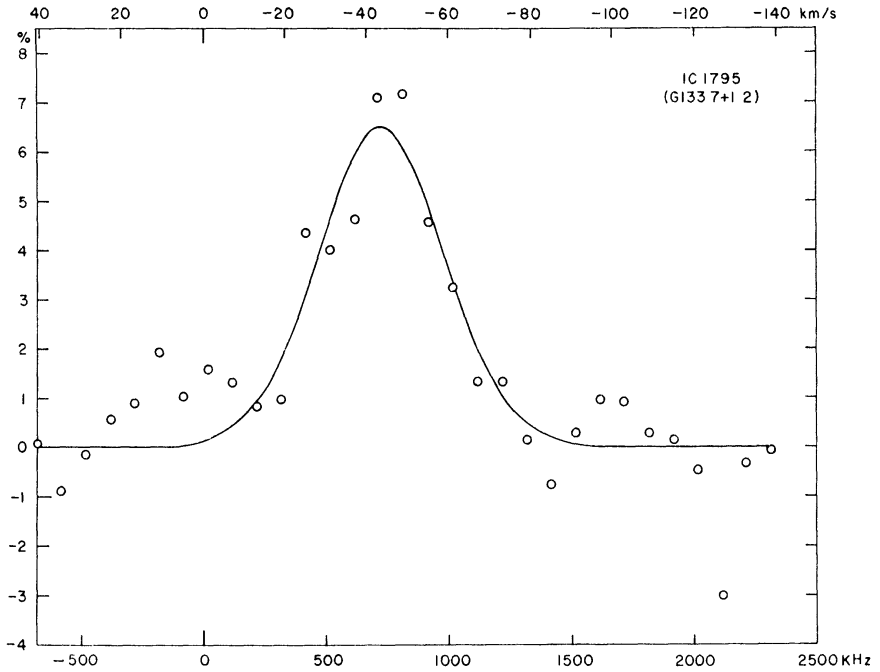

FIG. 1(1)

FIG. 1.—Hydrogen recombination 109α lines observed in galactic H II regions. The heavy curves are Gaussian profiles of best fit The outer points in the measured profiles have a lower statistical weight since their integration time is considerably shorter than the integration time of the center values. The spectra of Orion A and M17 have been shown in an earlier paper (Höglund and Mezger 1965). The indicated line temperatures have to be reduced by a factor 5.5/6 5. [In Fig. 1(9), the labeling is incorrect: *read* AMWW 39/W31 *instead of* AMWW 39/31]

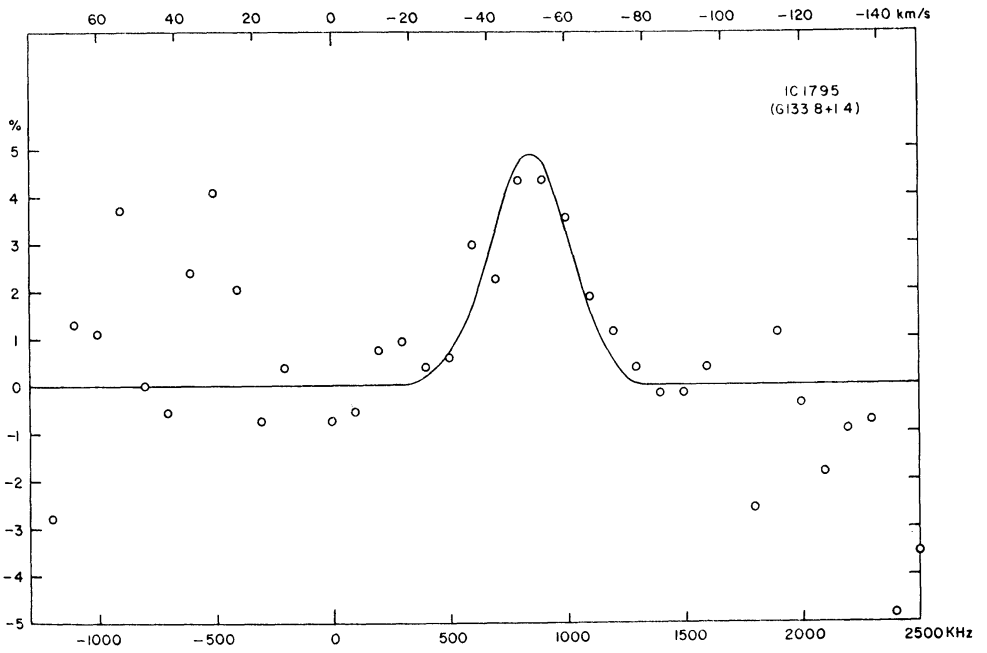

FIG. 1(2)

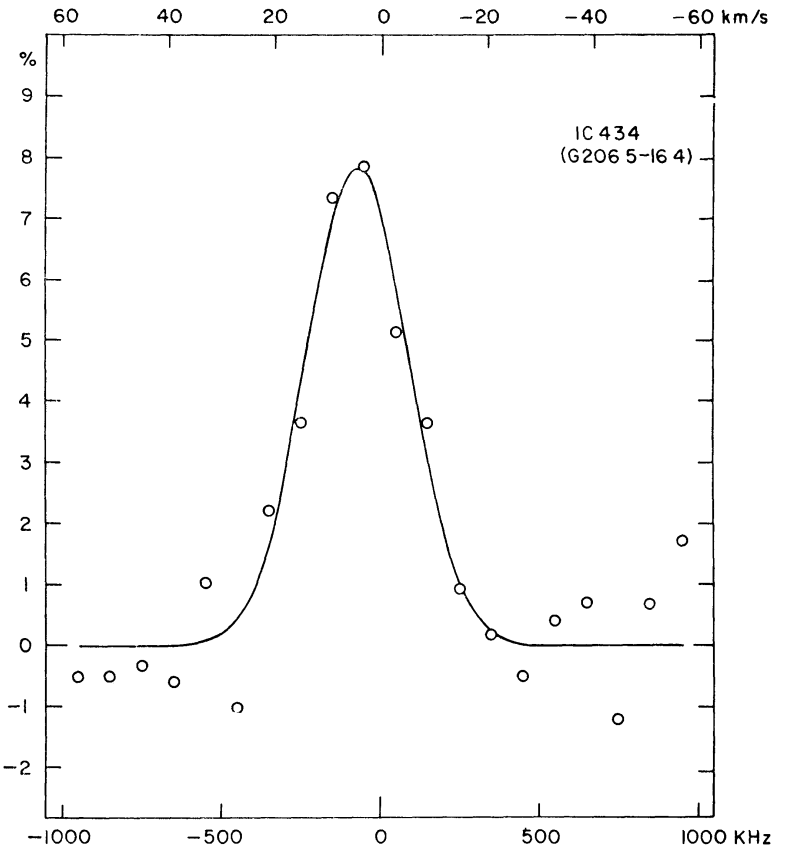

FIG. 1(3)

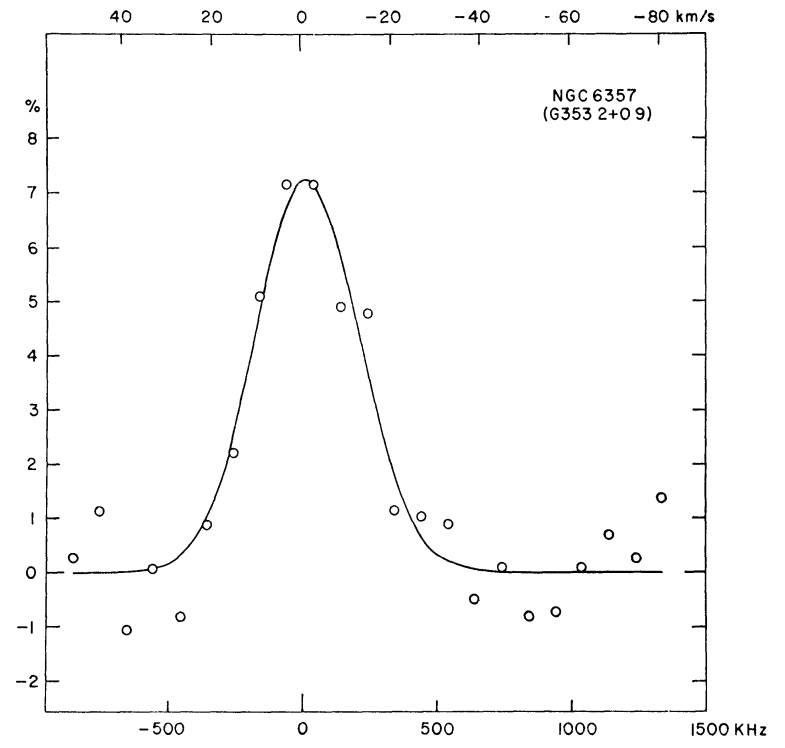

FIG. 1(4)

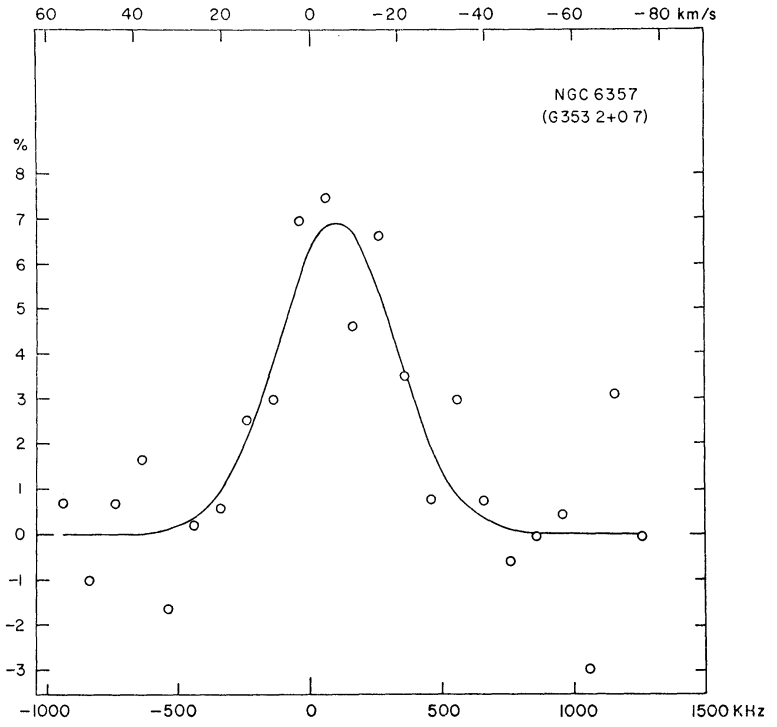

FIG. 1(5)

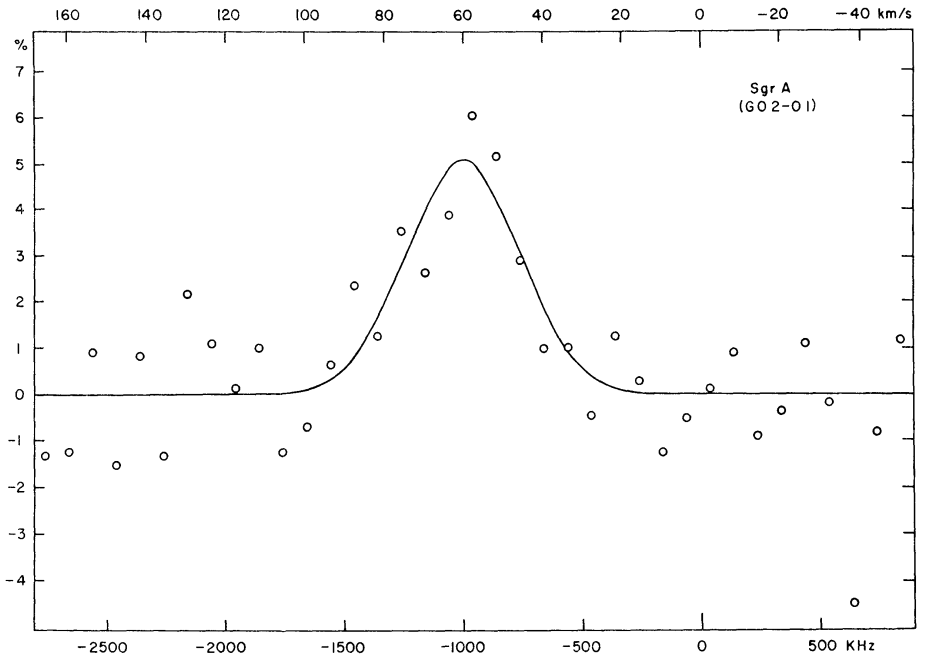

FIG. 1(6)

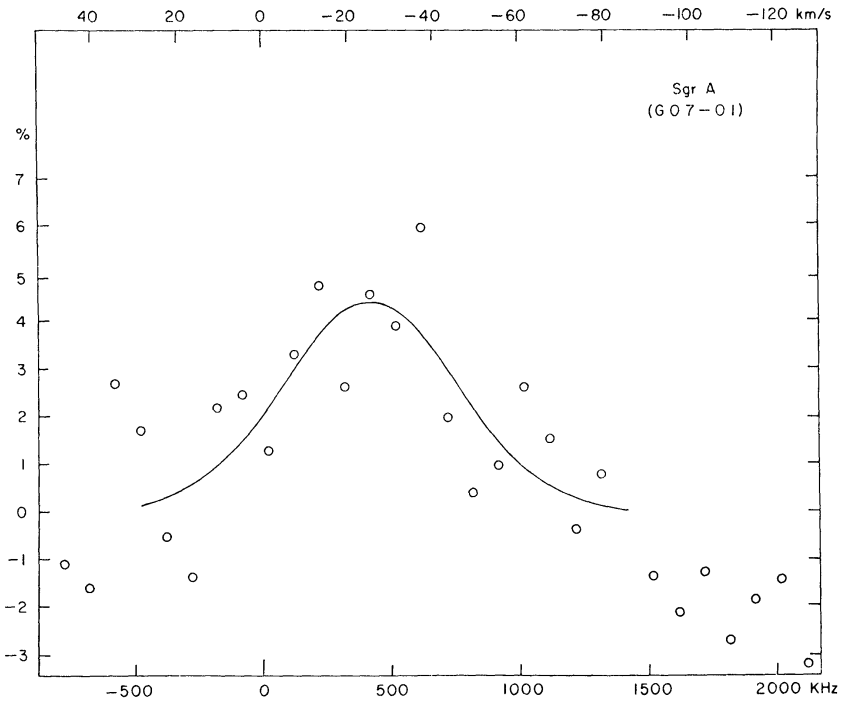

FIG. 1(7)

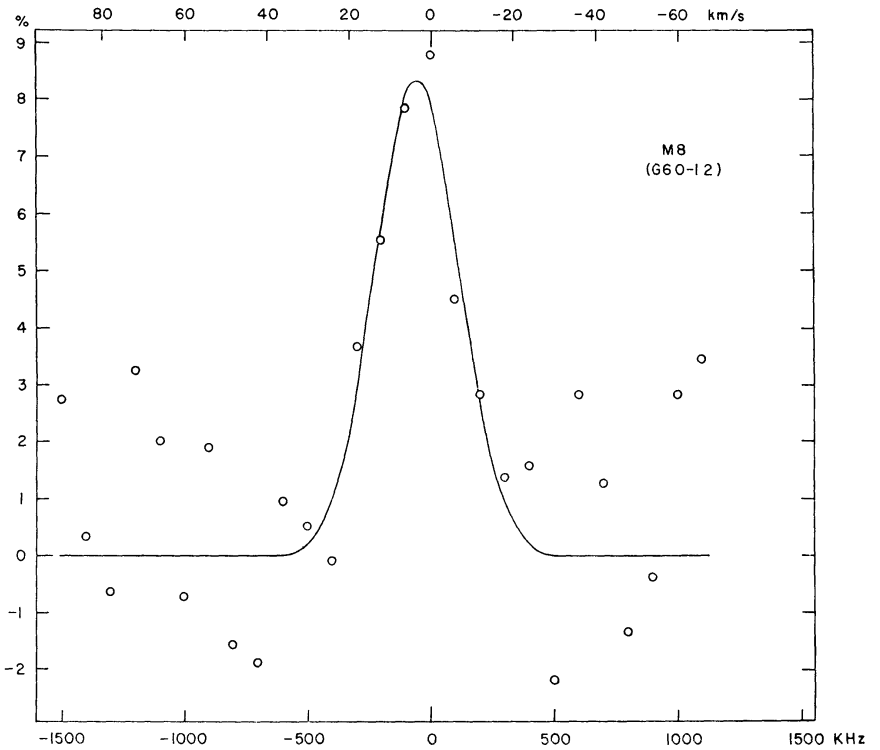

FIG. 1(8)

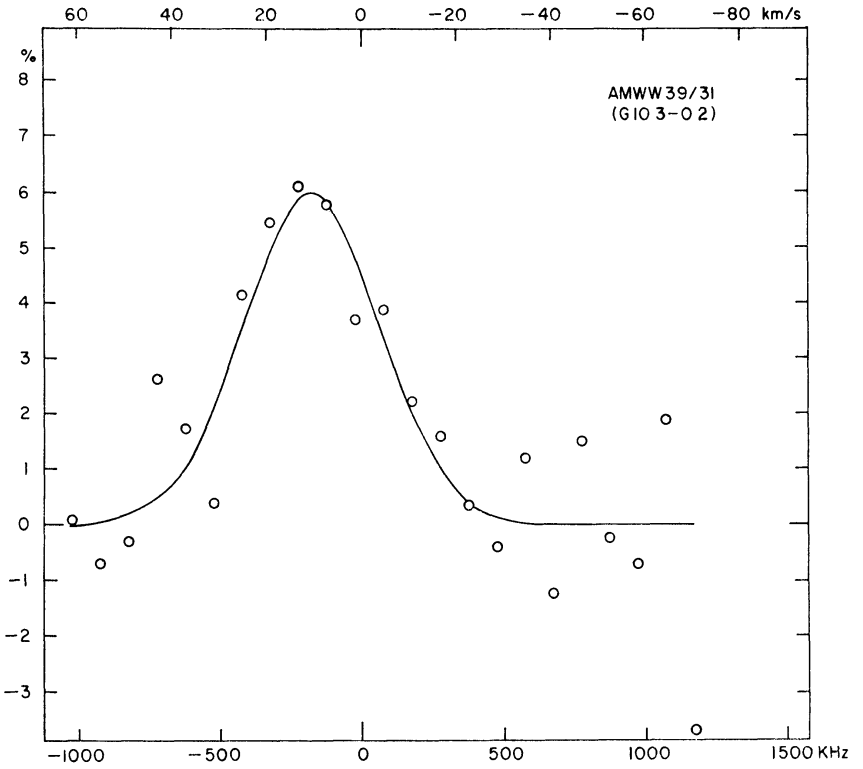

FIG. 1(9)

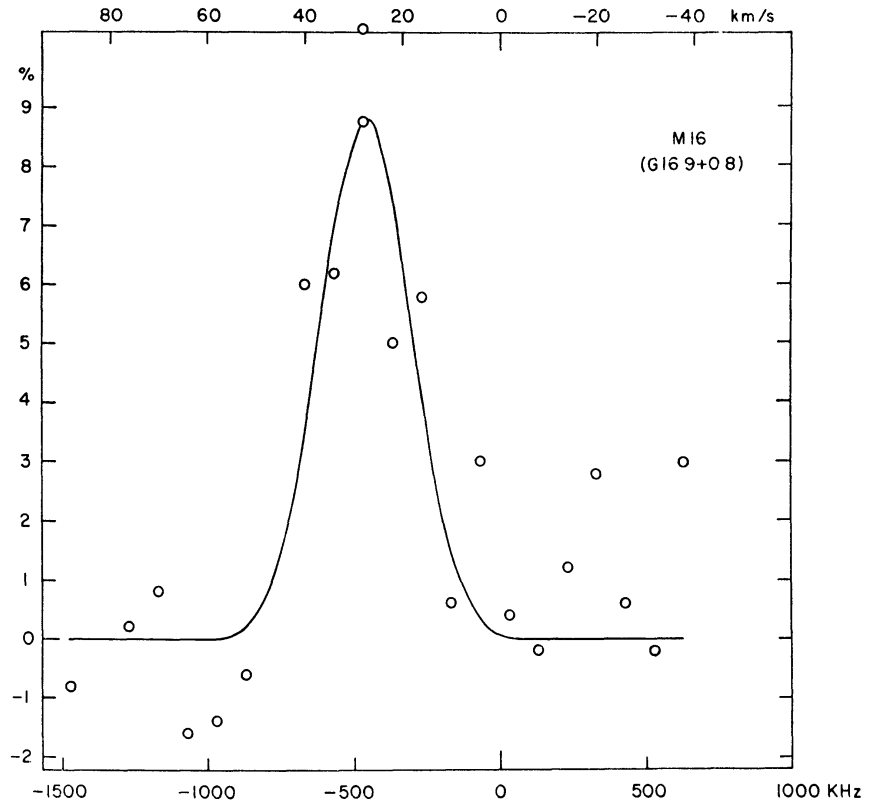

FIG. 1(10)

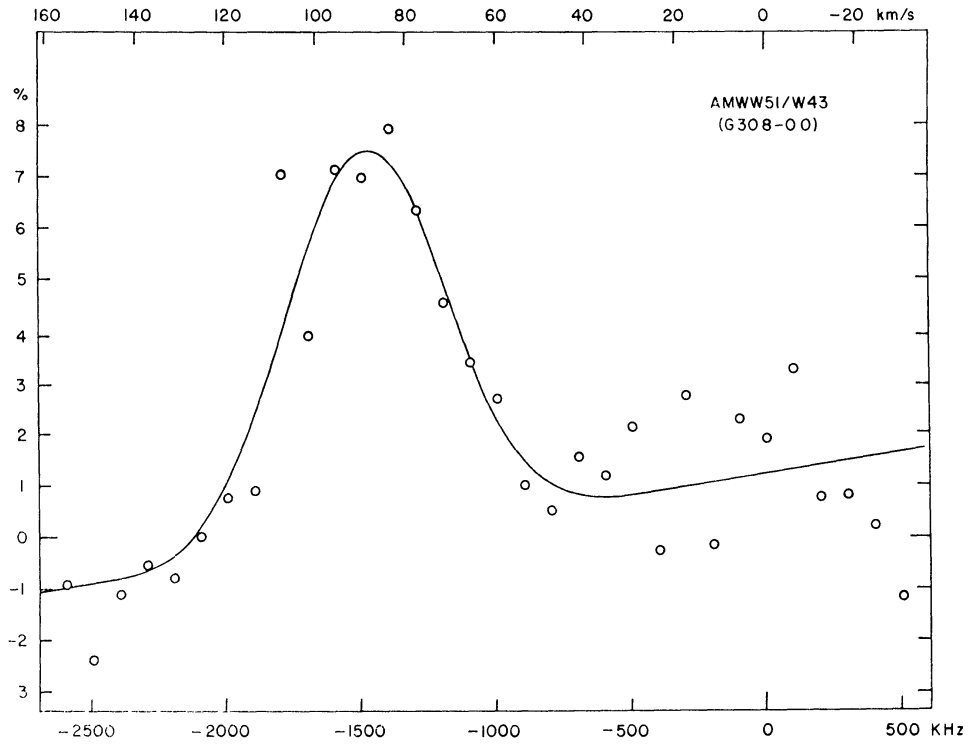

FIG. 1(11)

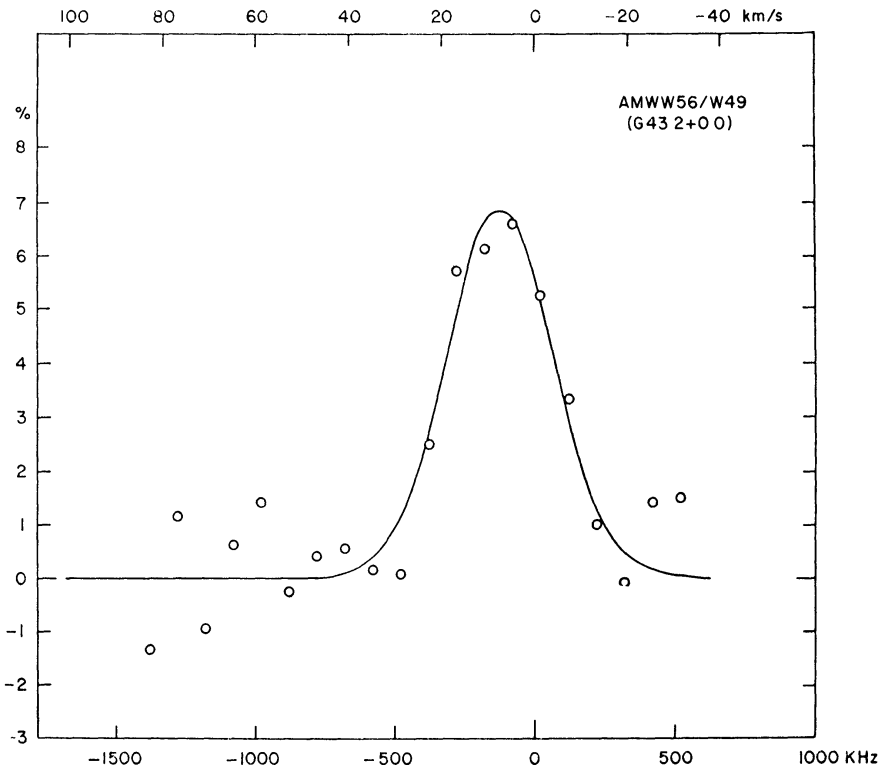

FIG. 1(12)

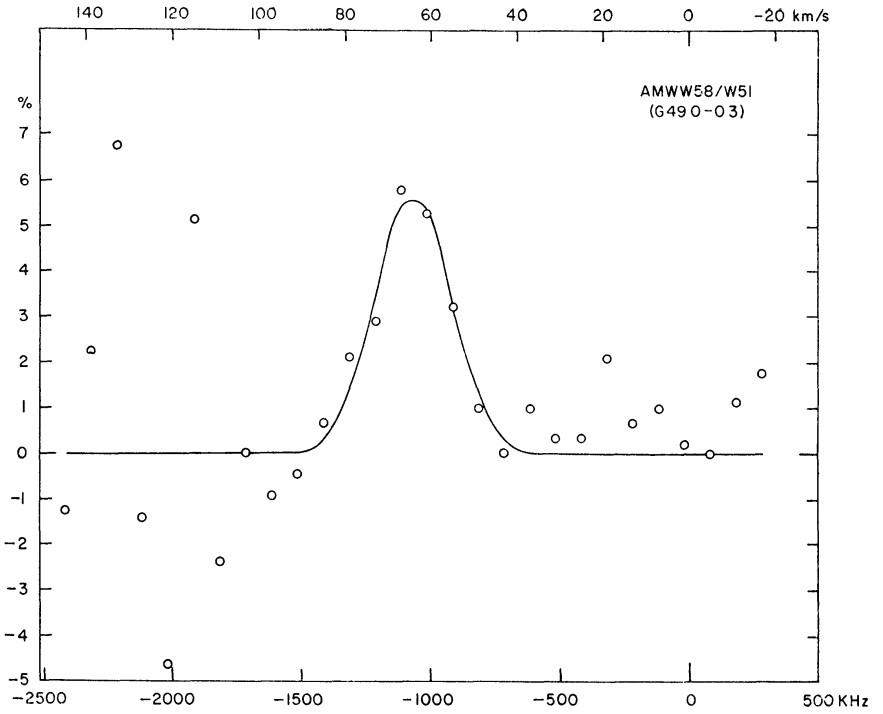

FIG. 1(13)

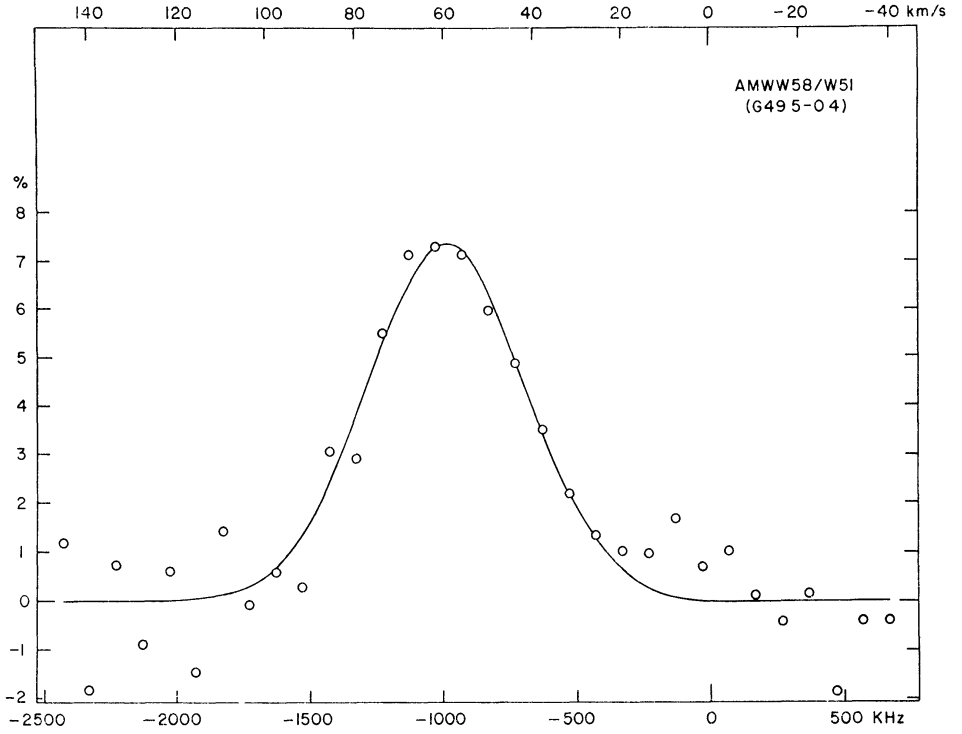

FIG. 1(14)

lowing as "AC") for distances $D \leq 3$ kpc. The parameters of this model are given by the International Astronomical Union (1963). All H II regions in our survey having distances $D > 3$ kpc are located in the inner part of the galactic system. In these cases we have used the galactic rotation curve as determined from 21-cm line observations (Kwee, Muller, and Westerhout 1954), but with the distance scale expanded, so that $R_0 = 10$ kpc. Since we are only using differences between the radial velocity of the Sun and the radial velocities of the H II regions (reduced to LSR), the older value of the galactocentric velocity of the Sun (assumed to be 216 km/sec in the paper of Kwee *et al.*) need not be changed.

Apart from systematic deviations of the galactic rotation from a circular motion, the kinematic distance determination may be incorrect due to random motions of the H II regions. To obtain an estimate of the rms velocity of the peculiar motion of H II regions, we have used the following method. In four cases where radial velocities of diffuse emission nebulae have been determined from both optical and radio observations, we found a good agreement between optical and radio data in three cases. A violent disagreement has been found only in the case of IC 434. But Campbell and Paddock (Campbell and Moore 1918) could not find any bright lines in this nebula during their survey, and it may be possible therefore that the radial velocity given by Courtès (1960) is caused by a confusion with another nearby H II region. We conclude that radio and optical measurements of the radial velocities of bright diffuse emission nebulae yield the same values. In Table 6, Appendix (see below), radial velocities and distances of twenty-eight H II regions have been compiled, and a statistical analysis yields a velocity dispersion for the radio data of 6.6 km/sec. The rms error in the determination of the radio radial velocities (Table 1, eighth col.) is 2.4 km/sec. Random motions of the H II regions and observational errors in the velocity measurements together yield an uncertainty of 7 km/sec on top of any systematic deviation of the galactic rotation from circular motion.

In such cases where two distances are compatible with an observed radial velocity, we removed the ambiguity in the kinematic distance determination by either comparing the kinematic distance with that distance derived from optical methods or—if no identification with an optically visible H II region is possible—by comparing the hydrogen recombination-line spectrum with the 21-cm line absorption spectrum of the investigated source. We lack such an information for only one object, W31.

The first column in Table 2 gives the name of the source; the second column its *G*-component in which the recombination line has been observed. The third column gives the optical distance; the references attached to these distances are the same as used in Table 6, Appendix. The fourth column gives the kinematic distances; in those cases where the radio sources are not identified with an optically visible H II region, we give both possible distances. The indicated errors of the kinematic distances come from the rms velocity of 7 km/sec of the peculiar motion of the H II regions. The fifth column gives the adopted distances which are used in Paper I for the computation of the total mass of ionized hydrogen and the electron density. These adopted distances are: (i) the optical distances in the cases where the optical distance lies within the errors of the kinematic distance; (ii) the limiting value of the kinematic distance which is closest to the optical distance in the cases where the optical distance lies outside the error brackets of the kinematic distance; (iii) the farther or closer kinematic distance depending on whether the 21-cm line absorption spectrum shows absorption at the maximum radial velocity of the expected profile, in the cases where the H II regions are not optically identified. It seems to be necessary to justify the adopted distances for some H II regions by an individual discussion.

IC 1795, G133.7 + 1.2; G133.8 + 1.2.—The lower limits of the radial velocities yield for the kinematic distances of the two components 2.4 and 2.8 kpc, respectively. We assume that both components are at the same distance and hence adopt the mean value of 2.6 kpc.

TABLE 2

DISTANCES, ELECTRON AND DOPPLER TEMPERATURES, AND RMS VELOCITIES OF INTERNAL TURBULENCE OF GALACTIC H II REGIONS*

SOURCE	RADIO COMPONENT	DISTANCE (kpc)				$\Delta\nu_D$ (kHz)	T_e (° K)	$\langle V_t^2\rangle_{rms}$ (km/sec)	T_D (° K)
		Optical	Kinematic		Adopted				
IC 1795	G133 7+1 2	2 42 (1)	$2\ 7^{-0\ 3}_{+0\ 3}$		2 6	586	5100^{+720}_{-1250}	23 2	26890
	G133 8+1 2		$3\ 1^{-0\ 3}_{+0\ 3}$		2 6	384	9450^{+1220}_{-2260}	7 2	11550
Orion A	G209 0−19 4	0 53 (1)	$0\ 0^{-0\ 0}_{+0\ 5}$		0 5	476	6400^{+680}_{-1500}	16 8	17740
	3′ north					450	5630^{+720}_{-1350}	15 9	15860
	3′ south					594	4880^{+520}_{-1170}	23 7	27630
	12′ west					776	3390^{+400}_{-800}	32 9	47150
	12′ east					469	6510^{+1230}_{-1620}	16 3	17220
IC 434	G206 5−16 4	0 4 (2)	$0\ 4^{-0\ 4}_{+0\ 6}$		0 4	362	6510^{+690}_{-1530}	9 6	10260
NGC 6357	G353 2+0 9	1 0 (5)	$0\ 4^{-0\ 4}_{+2\ 0}$		1 0	440	5950^{+630}_{-1400}	15 1	15160
	G353 2+0 7		$1\ 7^{-1\ 7}_{+1\ 9}$		1 0	519	5520^{+840}_{-1350}	19 6	21090
Sgr A	G0 2−0 1					564	6470^{+910}_{-1580}	21 4	24910
	G0 7−0 1					811	5550^{+910}_{-1360}	33 7	51500
M8	G6 0−1 2	1 1 (1)	$1\ 1^{-1\ 1}_{+2\ 3}$		1 1	392	5790^{+880}_{-1410}	12 4	12030
W31	G10 3−0 2		$2\ 1^{-1\ 3}_{+1\ 3}$	$17\ 8^{-1\ 2}_{+1\ 2}$	2 1	555	5730^{+670}_{-1370}	21 3	24120
M16	G16 9+0 8	1 7 (1)	$3\ 4^{-0\ 9}_{+0\ 9}$		2 5	353	5990^{+1130}_{-1490}	9 7	9760
M17	G15 0−0 7	1 8 (4)	$2\ 4^{-1\ 0}_{+0\ 9}$		1 8	636	4920^{+520}_{-1150}	25 7	31670
	3′ north					638	5330^{+690}_{-1280}	25 6	31870
	3′ south					498	5060^{+540}_{-1190}	18 9	19420
	12′.5 west					579	4830^{+520}_{-1130}	23 0	26250
	12′.5 east					537	5040^{+540}_{-1180}	20 8	22580
W43	G30 8−0 0		$6\ 5^{-0\ 7}_{+0\ 6}$	$10\ 7^{-0\ 7}_{+0\ 6}$	6 5	691	3970^{+420}_{-950}	28 8	37390
W49	G43 2+0 0		$0\ 5^{-0\ 5}_{+0\ 5}$	$14\ 1^{-0\ 5}_{+0\ 4}$	14 1	435	6310^{+740}_{-1510}	14 5	14820
W51	G49 0−0 3		$6\ 5^{-1\ 0}_{+1\ 0}$		6 5	332	9450^{+1550}_{-2310}		8630
	G49 5−0 4		$5\ 4^{-1\ 2}_{+1\ 2}$	$7\ 6^{-1\ 1}_{+1\ 2}$	6 5	689	3980^{+420}_{-930}	28 7	37170

* References: see Table 6

NGC 6357, G353.2 + 0.9; G353.2 + 0.7.—We assume that both components are at the same distance and adopt then the optical distance.

W31 (AMWW 39), G10.3 − 0.2.—No 21-cm absorption measurements are available for this source. We have not observed the line radiation of the components G10.2 − 0.3 and G10.6 − 0.4. We conclude from the angular extent of this H II region that the closer distance of 2.1 kpc is the correct value, provided that all three components belong to one H II region.

M16.—The 21-cm line absorption spectrum of this source shows absorption lines up to 35.9 km (Clark 1965). The radial velocity of 27.9 km/sec of this H II region can therefore hardly be explained as an unusually high peculiar motion. Also, Terzian (1965) gives a distance of 2.5 kpc for M16.

W43 (AMWW 51).—The 21-cm line profiles at the position of this source show absorption at the radial velocities +12 km/sec and between +64 and +94 km/sec. However, at +40 km/sec an emission feature is found which is narrowly confined in galactic latitude and therefore must belong to the far part of the Sagittarius arm (F. J. Kerr, private communication). Also, absorption does not extend up to the highest radial velocities at which emission occurs. Hence, we adopted the closer distance of 6.5 kpc.

W49 (AMWW 56), G43.2 + 0.0.—Akabane and Kerr (1965) find the 21-cm line in absorption at all positive radial velocities. We therefore, adopted the farther distance.

W51 (AMWW 58), G49.0 − 0.3; G49.5 − 0.4.—The 21-cm line observations (G. Westerhout; T. K. Menon and D. R. W. Williams, private communication) show absorption up to the highest radial velocities. Optical and radio observations agree that $l^{II} \approx 50°$ defines the tangential direction of a spiral arm (see, e.g., Kerr and Westerhout 1965). We therefore conclude that both components are located close to the point of maximum radial velocity at that direction, which occurs at the distance 6.5 kpc.

Becker and Fenkart (1963) have investigated the distribution of fifty-five H II regions in the vicinity of the Sun. Three sections of apparent spiral arms were found as rather sharply defined features. We have added to their distribution of H II regions (Fig. 2) those H II regions from our survey, which either are not included in Becker and Fenkart's paper or where our distance determination deviates from their optically determined distance (e.g., M16).

Kinematic distances of more H II regions have to be obtained before the few giant and distant H II regions found in this survey can be safely associated with any of the spiral arms in the vicinity of the Sun found by Becker and Fenkart. Preliminary results of our high-angular-resolution surveys show that the thermal disk component of the galactic continuum radiation breaks up into individual sources; these are probably distant H II regions. An extended recombination-line survey of these weak H II regions—which is well within the possibilities of modern radio telescopes and low-noise radiometers—should hence provide an independent method of studying the large-scale structure of our Galaxy.

IV. ELECTRON TEMPERATURE

We use Kardashev's (1959) equation (13) for the brightness temperature T_L in the line center in the form $\Delta\nu_L T_L = 1.677 \times 10^6 E T_e^{-1.5}$.[3] Dividing it by the approximation for the brightness temperature of the free-free continuum T_C given by equation (A.1b) of Paper I, we obtain

$$\left(\frac{\Delta\nu_L}{\text{kHz}}\right)\left(\frac{T_L}{T_C}\right) = 2.036 \times 10^4 \frac{1}{a(\nu,T_e)} \left(\frac{\nu_L}{\text{GHz}}\right)^{2.1} \left(\frac{T_e}{°\text{K}}\right)^{-1.15}; \qquad (2a)$$

$a(\nu,T_e)$ is a factor, given in Table 6 of Paper I for a large range of values of both T_e and ν. Substituting this factor allows us to evaluate equation (2a) with the exact formula for

[3] The numerical evaluation of Kardashev's equations is performed in this paper using the physical quantities quoted by Allen (1963)

the optical path length of free-free emission. In most practical cases we can set $a \approx 1$. In this equation ν_L is the center frequency and $\Delta\nu_L$ the Doppler width of the line. This equation has been derived under the assumptions that: (i) the excitation temperature of the line is equal to the electron temperature (thermal equilibrium); (ii) the H II region is optically thin in both line and continuum; (iii) the line shape is Gaussian.

If these assumptions are valid, we can compute the electron temperature of an H II region from the observed ratio of line to continuum brightness temperature multiplied by the line width. Substitution of $a(\nu,T_e) = 1$, $\nu = 5.009$ GHz in equation (2a) yields

$$\left(\frac{\Delta\nu_L}{\text{kHz}}\right)\left(\frac{T_L}{T_C}\right) = 6.00 \times 10^5\, T_e^{-1.15}. \tag{2b}$$

Inserting our observational results given in the sixth column of Table 1, we obtain the electron temperatures given in the seventh column of Table 2. The temperature values vary from 9450° K (IC 1795, G133.8 + 1.4) to 3970° K (W43), with a mean value of 5820° K (omitting the off-center values for Orion A, M17, and the electron temperature of W51, G49.0 − 0.3, since the free-free continuum of the latter source may be con-

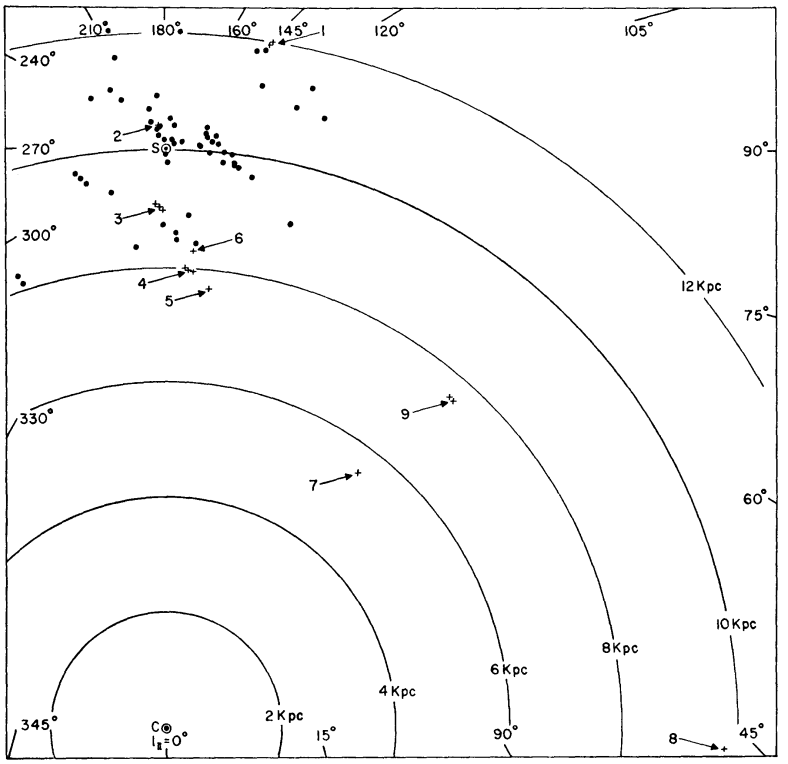

FIG. 2.—Distribution of H II regions, projected on the galactic plane (*open circles*, Becker and Fenkart 1963; *plusses*, this paper). (Note that 30° is mislabeled 90°.) The sources, whose kinematic radio distances have been used to construct this diagram, are tabulated below:

No	Source	Component
1	IC 1795	G133.7+1 2; G133 8+1 4
2	IC 434	G206 5−16.4
3	NGC 6357	G353.2+0.9; G353 2+0 7; G353 1+0 4
4	W31	G10 3−0 2; G10 2−0 3; G10 6−0 4
5	M16	G16 9+0 8
6	M17	G15 0−0 7
7	W43	G30 8−0 0
8	W49	G43 2+0 0
9	W51	G49 0−0 3; G49 5−0 4

taminated by non-thermal radiation). They are considerably lower than earlier estimates of the electron temperature of H II regions. There are, however, two more results of independent radio astronomical observations indicating considerably lower electron temperatures than derived from optical and earlier radio measurements.

Mills, Little, and Sheridan (1956) have observed H II regions at the wavelength 3.5 m, where the brightness temperature T_n of the non-thermal galactic background radiation close to the galactic plane exceeds 10^4 ° K. At this wavelength most of the investigated H II regions are optically thick. The emission nebulae are found either in emission or absorption, depending on whether the background temperature $T_n \lesseqgtr T_e$. M17 and NGC 6357 were found in absorption; from their determination of the absolute brightness temperature of the non-thermal radiation, Mills *et al.* estimated an electron temperature for NGC 6357 of 6500° K with an upper limit of 7800° K. Our line measurements yield a value of about 6000° and 5500° K, respectively (Table 2, seventh col.), for the two components of this H II region.

Menon (1961) used the turnover point in the broad-band radio spectrum of Orion to compute its electron temperature. We repeated these computations, but used improved spectra of both Orion A and IC 434 as well as models of the optical depths of both nebulae which are based on high-resolution contour maps derived from 2-cm observations with the NRAO 140-foot telescope (P. G. Mezger, Y. Terzian, and J. Schraml, in preparation). It is found that the electron temperatures of both nebulae must be considerably lower than 10000° K.

Such low electron temperatures have been predicted for spiral-arm galactic H II regions in a recent paper by Burbidge, Gould, and Pottasch (1963). It is of interest to note that these authors have determined the electron temperature of M8 from the observed optical line intensities O II/Hα and O III/Hα. They found a value of 5700° K and after correcting for reddening, 5800° K. Our line observations yield a value of about 5800° K for this nebula. Osterbrock (1965) has rediscussed the computations by Burbidge *et al.* He predicts electron temperatures of about 7000° K for diffuse nebulae. Even somewhat lower average electron temperatures have been computed by Hjellming (1966).

The discrepancy between the electron temperatures determined from optical and radio measurements may be due to the fact that optical measurements refer to the very brightest central parts of the H II region, whereas the radio observations yield an average value of the whole nebula. Our recombination-line observations at four points spaced by 3′ from the center of the Orion Nebula tend to support this explanation, although we find that the electron temperature remains remarkably constant over a similar 3′ region in M17 (see Table 2). A decrease of the electron temperature with increasing distance from the center of the Orion Nebula would also explain the low value of the electron temperature that we obtain from an analysis of the broad-band spectrum of this H II region ($T_e < 4000$° K). Hjellming's computations predict a general increase in electron temperature with increasing distance from the exciting star whenever the electron density is low enough so that collisional de-excitation effects are unimportant in determining the cooling rate of the plasma. In regions of higher electron density, however, the cooling becomes less effective due to collisional de-excitation (see Fig. 6 of Hjellming 1966). This causes the electron temperature to be higher than it would be under the same conditions, but at lower electron densities. Most of the H II regions investigated in our survey have bright central cores of relatively high density; a typical example is the Orion Nebula. Under these conditions Hjellming's computations predict a decrease of the electron temperature with increasing distance from the exciting star until the density becomes low enough. Then the electron temperature would rise again. Detailed recombination-line investigations of extended H II regions should yield experimental evidence.

V. ENHANCED LINE RADIATION DUE TO STIMULATED EMISSION

The electron temperature derived from the observed ratio of line to continuum brightness temperature depends on the validity of equations (2a) and (2b). Large systematic

errors in our brightness temperature measurements can be ruled out, since the evaluation of observations of other than the 109α line yields similar low electron temperatures (see Table 3, Fig. 4). The assumptions entering into the derivation of equations (2a) and (2b) are listed at the beginning of § IV. These assumptions will be discussed in this section in somewhat more detail.

Assumption i.—It has been assumed that the population of the energy levels of the hydrogen atom with the principal quantum number $n = 110$ and $n = 109$ is given by a Boltzmann distribution with a temperature equal to the electron temperature of the free electrons. A necessary (but—as will be seen in the following—not sufficient) condition for thermal equilibrium is that the b_n factors of these energy levels are close to unity. The b_n factor describes a departure from thermal equilibrium due to radiative processes. Values of the b_n factor for the range of principal quantum numbers $n \geq 40$ and for the electron temperature $T_e = 10^4$ ° K and electron density $N_e = 10^4$ cm^{-3} have been computed by Seaton (1964). For $n = 109$ his computation yields a value which is only a

TABLE 3

THE PRODUCT $\Delta\nu_L T_L/T_C$, OBSERVED FOR M17 AND ORION A AT VARIOUS Hα-RECOMBINATION LINES

Source	H Line	ν_L(MHz)	$\Delta\nu_L$/kHz	T_L/T_C	$\Delta\nu_L T_L/T_C$ (kHz)	Ref *
M17. .	94α	7792 9	1100 (± 4.5%)	6 6 ×10^{-2} (±14.6%)	72.6 (±15.7%)	(1)
Orion A	94α	7792 9	850 (±11 8%)	7 1 ×10^{-2} (±16 1%)	60 4 (±20 0%)	(1)
M17	109α	5008 9	643 (± 3 9%)	5 3 ×10^{-2} $\left(\begin{smallmatrix}+36\% \\ -\ 9\%\end{smallmatrix}\right)$	34 1 $\left(\begin{smallmatrix}+36\ 2\% \\ -\ 9\ 8\%\end{smallmatrix}\right)$	(2)
Orion A	109α	5008 9	485 (± 4 1%)	5 2 ×10^{-2} $\left(\begin{smallmatrix}+36\% \\ -\ 9\%\end{smallmatrix}\right)$	25 2 $\left(\begin{smallmatrix}+36\ 2\% \\ -\ 9\ 9\%\end{smallmatrix}\right)$	(2)
M17. . .	156α	1715 7	240 (±25 0%)	1 01×10^{-2} (±16 8%)	2 4 (±30 1%)	(3)
M17	158α	1651.5	230 (±26 1%)	1 15×10^{-2} (±14 8%)	2 6 (±30 0%)	(3)
M17	166α	1424 7	200 (±30 0%)	0 83×10^{-2} (±20 5%)	1 7 (±36 3%)	(4)

* References: (1) Meeks (1966, private communication); (2) Mezger and Höglund (1967); (3) Lilley *et al* (1966); (4) Palmer and Zuckerman (1966)

few per cent less than unity. Although the electron densities of the H II regions investigated here are considerably lower (87 cm$^{-3} \leq N_e \leq$ 1650 cm^{-3}) than the value used in Seaton's computation, we still believe that at the level $n = 109$ collisional processes are more important than radiative processes in establishing the level population, so that $b_{109} \approx b_{110} \approx 1$. Quantitative calculations are obviously needed to support our assumption.

Assumption ii.—It has been assumed that the H II regions are optically thin in both recombination line and free-free continuum. With τ_L, the optical depth in the center of the recombination line, and τ_C, the optical depth of the free-free continuum, this condition can be stated in the form $\tau_L \ll 1$; $\tau_C \ll 1$.

The condition $\tau_L \ll 1$ is certainly valid for all radio recombination lines. The condition $\tau_C \ll 1$ is valid at the frequency 5 GHz but is no longer valid at frequencies of 1.4 GHz or lower. The observed ratio of the excess line temperature $(T_{L+C} - T_C)$ to the continuum temperature T_C is related to the ratio T_L/T_C in equations (2a) and (2b) by

$$\frac{T_{L+C} - T_C}{T_C} = \frac{T_L}{T_C} \quad \text{for} \quad \begin{matrix}\tau_L \ll 1 \\ \tau_C \ll 1\end{matrix} \tag{3a}$$

$$= \frac{T_L}{T_C} \frac{\tau_C}{e^{\tau_C} - 1} \quad \text{for} \quad \begin{matrix}\tau_L \ll 1 \\ \tau_C \gtrsim 1.\end{matrix} \tag{3b}$$

If the condition $\tau_C \ll 1$ is no longer valid, the observed ratio of excess line to continuum temperature has to be multiplied by the factor $(e^{\tau_C} - 1)/\tau_C$ before the electron temperature can be computed from equations (2a) and (2b).

Assumption iii.—A Gaussian line shape is assumed. This assumption implies that Doppler broadening is the only mechanism effective in the broadening of the recombination lines. This assumption is certainly valid for the 109α line (see § VI).

On the basis of equation (3b) one would expect that with increasing optical depth τ_C the recombination lines merge more and more with the free-free continuum until for $\tau_C \gg 1$ they have completely disappeared. Equation (3b) has been derived for the case of thermal equilibrium. The assumption of thermal equilibrium, applied to the emission of radio recombination lines, has been questioned, however, in a recent paper by Goldberg (1966). Using Seaton's computation of the b_n factor, Goldberg shows that, although the ratio b_n/b_{n-1} is very close to unity, the derivative d/dn (ln b_n) is, in the radio frequency range, usually large as compared to the correction factor for stimulated emission $h\nu/kT_e$. This leads to a relative overpopulation of the upper level in the transitions $n \rightarrow (n - 1)$. The net effect of this slight departure from thermal equilibrium is an increase in the relative contribution of stimulated emission to the line intensity. Goldberg solves the equation of transfer treating the H II region as a homogeneous medium. In his notation r is the ratio of the excess line to the free-free continuum brightness temperature, including the contribution of stimulated emission to the line radiation; and r^* is the same ratio for thermal equilibrium only. He obtains

$$\frac{r}{r^*} = \frac{(\tau_C + \tau_L)/[\tau_C + (1-\gamma)\tau_L]\{1 - e^{-[\tau_C + (1-\gamma)\tau_L]}\} - (1 - e^{-\tau_C})}{[1 - e^{-(\tau_C+\tau_L)}] - (1 - e^{-\tau_C})}, \quad (4)$$

with $\gamma = d/dn$ (ln b_n) $kT_e/h\nu$.

This quantity is a measure of the enhanced line radiation due to stimulated emission; $r/r^* = 1$ corresponds to thermal equilibrium radiation. For a given recombination line the ratio r/r^* depends on both the optical depth τ_C of the free-free continuum and on the derivative (d/dn) (ln b_n). Goldberg estimates this latter quantity from Seaton's computed curves and predicts for the center of the Orion Nebula an enhancement of the line radiation of $r/r^* = 1.4$ (109α line) and 2.8 (166α line). If, in fact, $r/r^* > 1$ in the case of our observations the temperatures computed from equations (2a) and (2b) would be lower than the true electron temperatures of the H II regions. This obviously would affect the interpretation of our line observations discussed in §§ IV and VI. In the remainder of this section we therefore will compare our observational results with the predictions of Goldberg's theory.

For small values of the variables a series expansion of the exponential functions in equation (4) can be used, which we truncate after the quadratic terms. Neglecting small terms in sum expressions, the following approximation is derived:

$$\frac{r}{r^*} = 1 + \frac{\tau_C}{2}\gamma = 1 + \frac{\tau_C}{2}\frac{d(\ln b_n)}{dn}\frac{kT_e}{h\nu}, \quad (5)$$

which is valid under the conditions $(\tau_C + \tau_L) \ll 1$; $\tau_L \ll \tau_C$ and $|\tau_C + (1 - \gamma)\tau_L| \ll 1$, which apply for all our observations.

The dependence of the b_n factor on both electron temperature and electron density is not known for $n \geq 40$. As a simple working hypothesis we will assume that the derivative (d/dn) (ln b_n) is a quantity which varies only slowly with electron temperature and electron density in the ranges:

i) $n = 110$; $4000° \text{ K} \leq T_e \leq 10000° \text{ K}$; $80 \text{ cm}^{-3} \leq N_e \leq 1700 \text{ cm}^{-3}$

and which decreases with increasing principal quantum number no stronger than $\sim \nu$ in the range:

ii) $N_e \approx 565 \text{ cm}^{-3}$; $T_e \approx 5000° \text{ K}$; $94 \leq n \leq 167$.

Under these assumptions the ratio r/r^* at a given line frequency and for a given H II region is independent on the adopted electron temperature, since the product $\tau_C T_e$ is equal to the brightness temperature of the H II region, which is an observed and therefore fixed quantity. On the other hand, the quantity $(r/r^* - 1)$ is proportional to the optical depth τ_C of the free-free continuum, which can be approximated for the frequency and electron temperature range considered here by equation (A.1b) of Paper I.

If the line radiation were enhanced due to stimulated emission, we would expect to find a strong correlation between the electron temperatures computed from equations (2a) and (2b) and either the emission measure (at a given recombination-line frequency) or the line frequency (for a given H II region).

To search for such a correlation, we have plotted in Figure 3 the electron temperature determined from our line observations (Table 2, seventh col.) versus the corresponding emission measures (Paper I, Table 5, col. 10). In the case of enhanced line radiation due

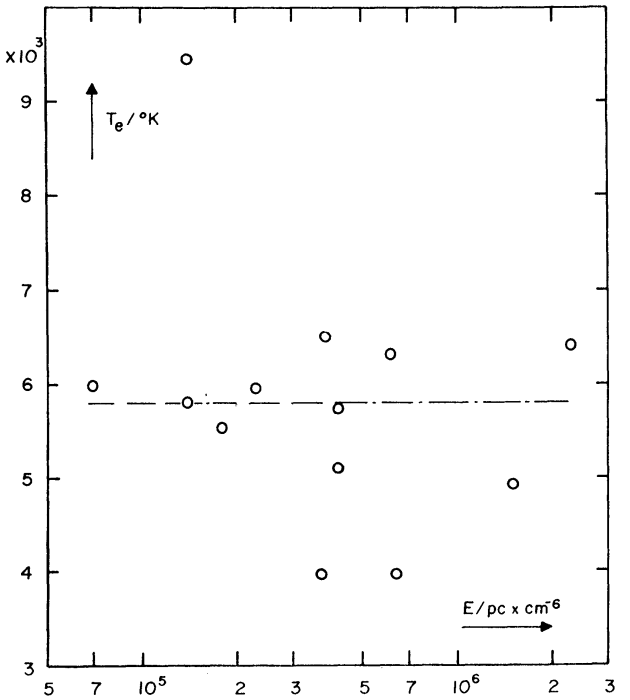

FIG 3.—Electron temperatures of H II regions, computed from eq. (2b) and plotted as a function of maximum emission measure. The dashed-dotted line corresponds to the average electron temperature $\langle T_e \rangle = 5820°$ K

to stimulated emission, we would expect a decrease in the electron temperature determined from our line observations with increasing emission measure. A very weak correlation may be present in the data of Figure 3. We cannot exclude, however, the possibility that the electron temperatures of M17 ($T_e = 4900°$ K), W43 ($T_e = 4000°$ K), and W51, G49.5 − 0.4 ($T_e = 4000°$ K) are too low due to the following reason. High-angular-resolution measurements have clearly shown that these three sources are associations of two or more H II regions with approximately equal intensity. If these components have somewhat different radial velocities, the observed product $\Delta v_L T_L$ will be too large since it has been determined under the assumption that the line profile has a single Gaussian shape. This will then yield too low an electron temperature.

In Figure 4 we have plotted the product $\Delta v_L T_L / T_C$, which is related to the electron temperature by equation (2a), as a function of line frequency. The observations have been made for M17 and the Orion Nebula by various observers. Their results, which

have been used to construct the diagram (Fig. 4), are compiled in Table 3. The straight lines in the diagram correspond to the case of thermal equilibrium as given by equation (2a), with the electron temperature as the parameter. The agreement between the observations made at various recombination lines is remarkably good, especially if the low-frequency values obtained for M17 by the Harvard group are increased by about 20–30 per cent according to equation (3b). If enhanced line radiation due to stimulated emission were effective in this frequency range, we would expect a deviation, at lower frequencies, of the observed values $\Delta\nu_L T_L/T_C$ in the direction of decreasing electron temperature.

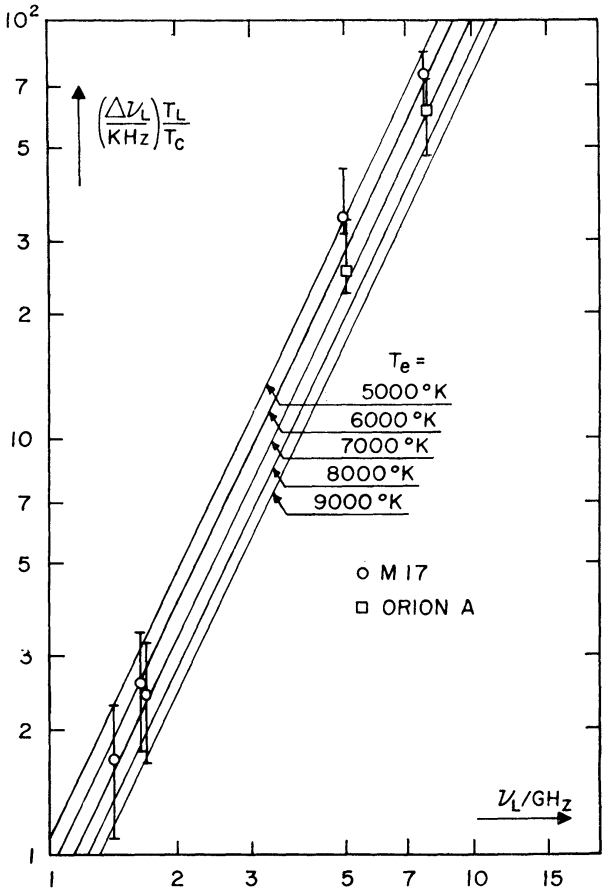

FIG. 4.—The quantity (line width $\Delta\nu_L$) × (ratio of excess line to free-free continuum temperature T_L/T_C) observed in M17 and Orion A at various recombination *na* lines. Measured values and observers are given in Table 3.

In the ninth column of Table 2 the observed line widths have been expressed by equivalent Doppler temperatures, using the relation equation (6b). In the case of thermal equilibrium, the Doppler temperature must always be equal to or larger than the electron temperature given in the seventh column of the same table. This condition is fulfilled in all cases except W51, G49.0 — 0.3; but in this particular case, we know that the electron temperature, as derived from equation (2b), is too high since the non-thermal radiation of a nearby source has been partly added to the free-free continuum of the H II region.

The assumption of a constant value d/dn (ln b_n), independent of electron density and decreasing no stronger than $\sim \nu$ with the principal quantum number, is certainly only a very crude approximation. We feel, nevertheless, that the diagrams of Figures 3 and 4

give strong evidence against an enhanced line radiation within the limits of electron density and principal quantum number where reliable observations have been made. In order to compare Goldberg's theory with observations, we need both more accurate computations of the b_n factors and more accurate recombination-line measurements especially at lower frequencies.

VI. INTERNAL TURBULENCE

We have mentioned in our first paper (Höglund and Mezger 1965) that the shapes of the recombination lines observed in M17 and in the Orion Nebula are well approximated by a Gaussian line profile, indicating that only Doppler broadening is significant in the observed line shapes. This conclusion was later confirmed, when the 156α and 158α lines (Lilley, Menzel, Penfield, and Zuckerman 1966) and the 166α line (Palmer and Zuckerman 1966) were detected in the same H II regions. It was found that even at the lowest frequency, 1424 MHz, the half-power width of the recombination line observed in M17 still decreases linearly with the line frequency. As has been noted by us and other observers, this experimental result contradicted Kardashev's (1959) estimate of the influence of Stark broadening on the radio recombination lines. Griem (1967) in a recent paper has rediscussed the Stark broadening of hydrogen $n\alpha$ recombination lines with large principal quantum numbers. He could show that under the physical conditions prevailing in the investigated H II regions (average electron densities $N_e = 10^2 \ldots 2 \times 10^3$ cm^{-3}; electron temperatures $T_e = 4 \times 10^3 \ldots 10^4$ ° K) most of the Stark broadening is due to inelastic electron collisions because ion and elastic electron collision broadening is much reduced by a near-cancellation of upper- and lower-state perturbations. Griem computes for the ratio of the Stark (electron collision)-broadened line half-power width $\Delta\omega_{ce}$, which in its far wings can be approximated by a Lorentzian line shape, to its Doppler half-power width $\Delta\omega_D$.[4]

$$\frac{\Delta\omega_{ce}}{\Delta\omega_D} = \frac{1}{0.6006}\,\frac{3}{2}\sqrt{\pi}\,\frac{\hbar c}{m}\,a_0^2\left(\frac{m}{kT_e}\right)^{1/2}\left(\frac{M_{\rm H}}{kT_D}\right)^{1/2} N_e n^7\left[\tfrac{1}{2} + \ln\left(\frac{kT_e}{E_{\rm H}}\,n\right)\right]. \tag{6a}$$

In this equation $\hbar$ is Planck's constant divided by 2π, c the velocity of light, m the electron mass, a_0 the Bohr radius, k the Boltzmann constant, $M_{\rm H}$ the mass of the hydrogen atom, T_e the electron temperature, N_e the electron density, n the principal quantum number, and $E_{\rm H}$ the hydrogen ionization energy (cgs units). The effective Doppler temperature in equation (6a) is defined by

$$T_D = (\Delta\nu_D)^2\,\frac{\lambda^2 M_{\rm H}}{8 \ln 2\, k}; \tag{6b}$$

it allows for any additional Doppler broadening of the observed lines due to internal turbulence in the H II region. This equation has been evaluated for the Orion Nebula ($T_e = 6400°$ K, $T_D = 1.77 \times 10^4$ ° K, $N_e = 1649$ cm^{-3}) and M17 ($T_e = 4900°$ K, $T_D = 3.17 \times 10^4$ ° K, $N_e = 565$ cm^{-3}) and the result is plotted in Figure 5. The electron impact broadening should become significant in the case of the Orion Nebula only for the 166α line. This line has, however, only been detected in M17 to date, where the predicted Stark width is only 0.40 of the Doppler width.

Since the line broadening is due only to Doppler broadening, if we know the electron temperature, we may compute the rms velocity $\langle v_t^2\rangle_{\rm rms}$ of the internal turbulence using the relation

$$\Delta\nu_D = \frac{2\nu_L}{c}\left[\ln 2\left(\frac{2kT_e}{M_{\rm H}} + \tfrac{2}{3}\langle v_t^2\rangle\right)\right]^{1/2}. \tag{7}$$

[4] The following equation differs from Griem's original equation by the factor 1/0.6006 which we have introduced to compare half-power widths of both Doppler and Stark profiles rather than the "half" half-power width of the Stark profile to the (1/e)-width of the Doppler profile.

The Doppler width $\Delta\nu_D$, given in Table 2, sixth column, is equal to the observed line width $\Delta\nu_L$ given in the fifth column of Table 1, after correction for the square-shaped radiometer band width $\Delta\nu_R = 95$ kHz by means of the relation

$$\Delta\nu_D = \Delta\nu_L\,[1 - (0.94\,\Delta\nu_R)^2/(\Delta\nu_L)^2]^{1/2}\,. \tag{8}$$

For T_e, the electron temperature of the H II region, we used the temperature values of the seventh column of Table 2, computed from the observed line-to-continuum ratios by means of equation (2b).

The rms velocities of the investigated H II regions are given in the eighth column of Table 2; their values range from 7.2 km/sec (IC 1795, G133.8 + 1.2) to 33.7 km/sec

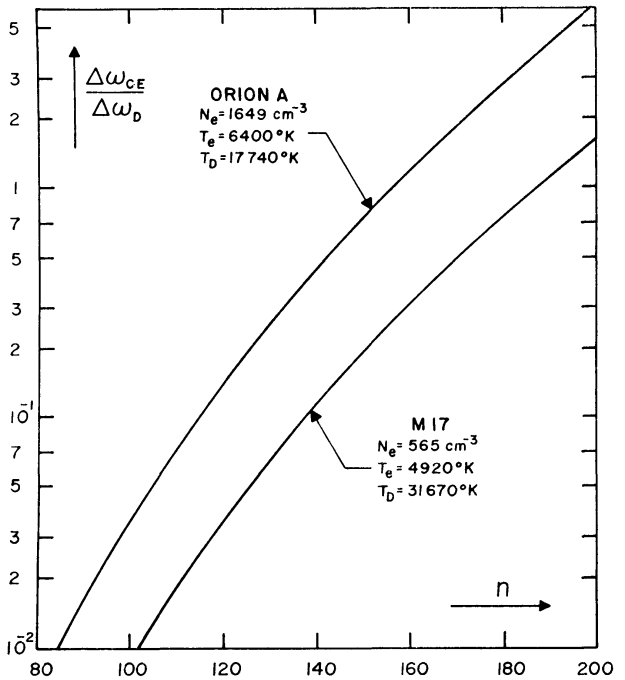

FIG. 5 —Ratio of Stark HPW to Doppler HPW for the recombination $n\alpha$ lines. The curves are computed for the physical conditions prevailing in Orion A and M17, using Griem's (1966) results.

(Sgr A, G0.7 − 0.1) with a mean value for fifteen H II regions of $\langle\langle v_t^2\rangle_{\rm rms}\rangle = 19.25$ km/sec (omitting again the value of W51, G49.0 − 0.3 for the reasons mentioned in § IV, as well as the off-center values of Orion A and M17).

The fact that the rms turbulence velocities in most H II regions thus far investigated are considerably larger than the velocity of sound (about 9 km/sec at $T_e = 5800°$ K) implies the existence of shock waves in the plasma. Since this conclusion might not be generally accepted, we compare the rms turbulence velocities obtained from our observations for the Orion Nebula (16.8 km/sec in the center and 15.9, 23.7, 32.9, and 16.3 km/sec for points spaced about 3′ from the center in directions north, south, west, and east) with optical measurements of the same parameter.

Baade, Goos, Koch, and Minkowski (1933) determined the turbulence velocities of the Orion Nebula at various positions by comparing the Doppler width of two O III lines (λλ5007 and 4959 Å) with the Doppler width of the Hβ line, eliminating in this way the pure thermal contribution to the observed Doppler widths. Their quoted velocity values have to be increased by a factor of 2 due to an erroneous formula used in their reduction (Minkowski 1934). In order to convert their mean velocity into the corresponding rms

velocity, we use the relation $\langle v^2 \rangle_{\rm rms} = \sqrt{(v^2\, 3\pi/8)}$. From their Figures 12 and 13, von Hoerner (1951) estimated

$$\langle v_t^2 \rangle_{\rm rms} = \begin{cases} 19.5 \text{ km/sec} & \text{close to the Trapezium} \\ 10.9 \text{ km/sec} & \text{outside} . \end{cases}$$

A very detailed spectrographic investigation of the Orion Nebula has been made by Wilson, Münch, Flather, and Coffeen (1959). The authors conclude from the analysis of their observations that the turbulence in the nebula consists of energy-containing waves, moving with supersonic velocities, which decay into subsonic eddies.

Goldberg (1965) has computed the Doppler broadening due to both thermal and turbulence effects from the observed number of members of the Balmer series, i.e., from the value of the principal quantum number n, at which the Doppler line width in the Balmer series just equals the separation between successive members of the series. Using the observations by Kaler, Aller, and Bowen (1965), he determines $n_{\rm max} = 39.5$ (i.e., the lines with $n = 39$ and $n = 40$ just merge) and obtains for the combined most probable velocity $v = \sqrt{(v_{\rm th}^2 + v_t^2)} = 23.5$ km/sec. An electron temperature $T_e = 6400°$ K yields a thermal velocity of $v_{\rm th} = 10.3$ km/sec. In order to convert the most probable velocity into the corresponding rms velocity, we multiply by $\sqrt{\frac{3}{2}}$ and obtain

$$\langle v_t^2 \rangle_{\rm rms} = 25.9 \text{ km/sec} .$$

Evidently both optical and radio measurements agree in yielding supersonic turbulence velocities for the Orion Nebula.

VII. IDENTIFICATION OF THERMAL AND NON-THERMAL SOURCES: THE GALACTIC CENTER

The detection or non-detection of recombination lines leads to an unambiguous identification of thermal and non-thermal galactic radio sources. In this manner we found that the component G43.3 − 0.2 in W49 is a non-thermal source which—if located at the same distance as the thermal component G43.2 + 0.0—has at $\lambda = 6$ cm an intrinsic radiation output similar to that of Cassiopeia A.

In the case of W51 the separation between thermal and non-thermal sources is not so clear. High-angular-resolution observations at $\lambda = 2$ cm show that there are at least four thermal components in this source. The recombination-line radiation of two of these components, G49.0 − 0.3 and G49.5 − 0.4, has been detected in our survey. The other two thermal components are distributed roughly along a line which connects the peaks of the thermal components mentioned above. (Their approximate positions are indicated in the contour map of W51 in Paper I, Fig. 1, by oblique arrows.) The non-thermal source seems to be rather extended, engulfing the thermal component G49.0 − 0.3. At frequencies of 750 MHz and lower where the non-thermal radiation is preponderant, the bulk of the observed radiation comes from a source whose declination is about +14°06′.

In the strongest source in the Cygnus X region, W75, we could not detect the line in the radial velocity range -108 km/sec $\leq v_r$(LSR) ≤ 186 km/sec although its broad-band spectrum indicates a thermal radiation mechanism (H. Wendker 1966). Our results are, however, marginal.

The strongest sources of the Sagittarius region have been investigated for their recombination-line radiation. Figure 6 shows a contour map of that region, obtained with the Australian 210-foot telescope at Parkes (Broten, Cooper, Gardner, Minnett, Price, Tonking, and Yabsley 1965) at $\lambda = 6$ cm. The line radiation of the four components indicated in this contour map has been investigated. The results are summarized in Table 4.

The central source is evidently a non-thermal source, in agreement with conclusions drawn from its broad-band spectrum (Maxwell and Downes 1964; Hollinger 1965). We

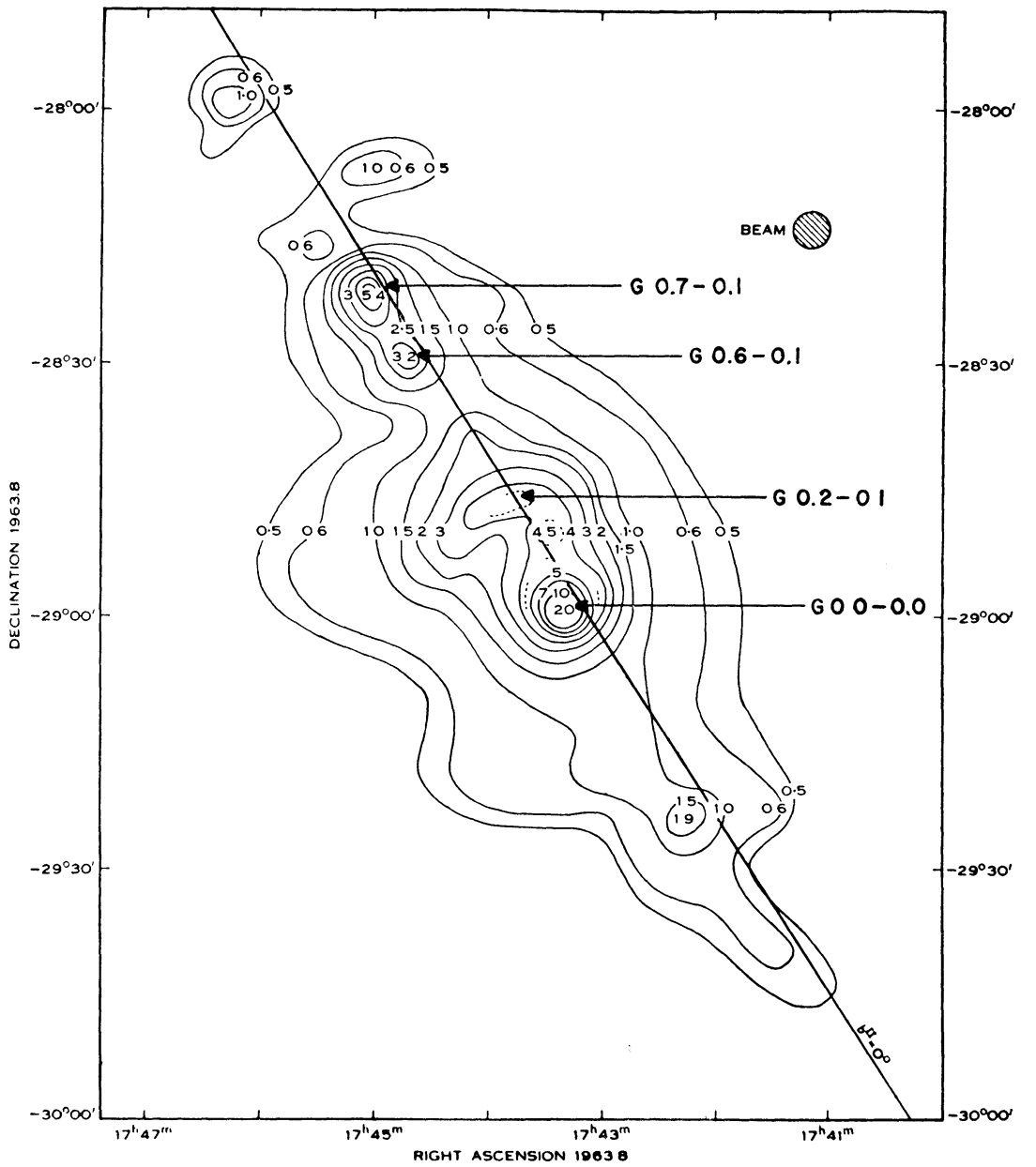

FIG. 6.—Contour map of the Sagittarius region, observed at $\lambda = 6$ cm with the Australian 210-foot telescope (Broten *et al.* 1965). The arrows indicate the source components whose 109α line radiation has been investigated.

TABLE 4

RESULTS OF A LINE SURVEY OF THE SAGITTARIUS REGION

Source Component	v_r(LSR) (km sec^{-1})	T_e(° K)	$\langle v_t^2 \rangle$ rms (km sec^{-1})	Analyzing Range
G0 0−0 0	. .	. . .	. .	$-87 \leq v_r \leq +141$ km sec^{-1}
G0 2−0 1	+59 4	6470	21 4	. . . .
G0 6−0 1	.	. . .	. . .	$-50 \leq v_r \leq +70$ km sec^{-1}
G0 7−0 1	−24 9	5550	33 7	. . .

could not find the recombination line in component G0.6 — 0.1, although this negative result is not too well established.

The two thermal components have radial velocities which can be hardly explained by galactic rotation. They show the 21-cm line radiation of the 3-kpc arm in absorption (F. Kerr, private communication) and therefore seem to be located close to the galactic center. The positive radial velocity of 59.4 km/sec for component G0.2 — 0.1 may be explained by assuming that this H II region partakes in the rotation of the central disk of neutral hydrogen (Rougoor and Oort 1960). The negative radial velocity of component G0.7 — 0.1 may be explained if this H II region partakes in the expansion of the 3-kpc arm. It would have a somewhat lower expansion velocity and seems to be located somewhere between the 3-kpc arm and the galactic center.

TABLE 5

RADIAL VELOCITIES OF OH EMISSION LINES AND THE HYDROGEN-RECOMBINATION LINES OF NEARBY H II REGIONS

SOURCE	COMPONENT	v_r(LSR) (km sec^{-1})		REF *	v_r(H II) − $\langle v_r(\mathrm{OH})\rangle$ (km sec^{-1})	$\langle[v_r(\mathrm{OH}) - v_r(\mathrm{H\ II})]^2\rangle_{\mathrm{rms}}$ (km sec^{-1})
		H II Region	OH Emission Line 1665 MHz			
IC 1795	G133 7+1 2	−43 5	−44 5; −45 7; −43 0; −43 9; −41 1; −48 4; −42 3; −40 5; −46 8; −47 8	(1)	+ 0 9	2 9
Orion A	G209 0−19 4	− 2 0	+20 9; +22 7; +6 9; + 4 4; +3 3; −5 4	(1)	−10 8	16 1
Sagittarius A	G0 2−0 1†	+59 4	+68 2	(2)	− 8 8	
W49	G43 2+0 0	+ 7 4	+16 8; +16 1; +20 9; +18 0; +17 6; +12 2; + 5 2; +13 7; +20 0; + 7 7; +11 2; + 3 4; +22 0	(1)	− 6 8	9 3
W51	G49 5−0 4	+59 1	+58 1; +59 5; +61 8	(1)	− 0 7	2 1

* References: (1) Weaver, Dieter, and Williams (1966); (2) McGee, Robinson, Gardner, and Bolton (1965)

† *Note added in proof:* Precise measurements of the position of the OH emission center in the Sagittarius region have meantimes shown that its position coincides rather with the thermal component G0 7−0 1, which has the radial velocity −25 km/sec

Although both H II regions seem to be rather close to the galactic center, their electron temperatures are hardly different from the electron temperatures found for spiral-arm H II regions. This indicates that even in the vicinity of the galactic center radiation ionization rather than collision ionization is the effective process in the formation of H II regions. Otherwise one would expect considerably higher electron temperatures (Burbidge *et al.* 1963).

VIII. THE RECOMBINATION LINE OF THE HELIUM ATOM

Kardashev (1959) has pointed out that recombination lines similar to those of the hydrogen atom should also be found for the helium atom. The helium line 109α has a frequency of 5010.970 MHz. Although Kardashev did not compute oscillator strength and population number for the helium atom, he estimated that these quantities should be rather similar to those of the hydrogen atom. We searched for this line in both the Orion and Omega Nebulae (eleventh col., Table 1) without success. If we consider a detection limit for the He line of three times the rms value quoted in Table 1, our nega-

tive result does not contradict the detection of the 166α He line by the Harvard group (Zuckerman 1966).

IX. CORRELATION WITH OH OMISSION

Weaver, Williams, Dieter, and Lum (1965) found that the OH line occurs in emission only at close angular distances from radio sources which are either optically identified with emission nebulae or whose broad-band spectrum suggests that they are H II regions. We investigated the correlation of the radial velocities of OH clouds with the radial velocities of nearby H II regions, which are obtained from their hydrogen-recombination line. The results are listed in Table 5.

The third column gives the radial velocity of the H II region referred to the local standard of rest as determined from the recombination-line observations. The fourth column gives the radial velocities of the OH clouds which are probably associated with the H II regions listed in the first two columns. The radial velocities of the OH emission lines given in the fourth column have been determined by Weaver, Dieter, and Williams (1966) (with one exception). The sixth column gives the difference between the radial velocity of the H II region and the mean velocity of the OH clouds; the seventh column gives the velocity dispersion between H II regions and associated OH clouds. The weighted mean value of the velocity dispersion determined for the five investigated H II regions is 7.9 km/sec. These results give strong support to the hypothesis that such OH clouds emitting the line are closely associated with H II regions.

We want to thank F. Kerr (CSIRO, Sydney, Australia), T. K. Menon (NRAO), and G. Westerhout (University of Maryland), who provided us with unpublished 21-cm line data. We also want to thank L. Goldberg (Harvard College Observatory), H. Griem (University of Maryland), and N. Dieter (University of California, Berkeley), who made their manuscripts available to us prior to publication. It is a pleasure to thank J. Schraml for his help in the reduction and discussion of our observations and to thank the operators and mechanics of the NRAO 140-foot telescope, without whose assistance we could not have performed our line survey.

APPENDIX

PECULIAR MOTION OF H II REGIONS

In Table 6 radial velocities and distances have been compiled for those H II regions which are optically identified. The heliocentric radial velocities are given in column 8; the references (figures in brackets following the velocity values) refer to the optical observations of Courtès (2) and the Lick Observatory (7) and to our own radio observations (6).

The distances of the H II regions obtained from optical observations (both photometric and spectroscopic) are given in column 7. In order to get as many distances as possible, we had to use values given by five authors. The distances assigned by these authors were given the following priorities:

i) Becker and Fenkart (1963), ref. (1), 14 distances
ii) Courtès (1960), ref. (2), 6 distances
iii) Pottasch (1965), ref. (3), 1 distance
iv) Allen (1963) (as quoted from different sources), ref. (4), 4 distances
v) Cederblad (1946), ref. (5), 2 distances

These distances were converted in radial velocities using the Australian Conference Model (col. 9) and the Howard-Kirk (1965) Model (col. 10) of galactic rotation. The absolute values of the differences between observed and computed radial velocities are given in column 11. The sign of the velocity deviations given in column 11 has been obtained by computing the kinematic distance from the observed radial velocities D_k and comparing this value to the optical distances given in column 7. A negative value of the difference $D_{opt} - D_k$ corresponds then to a

References (1) Becker and Fenkart, 1963; (2) Courtes, 1960; (3) Pottasch, 1965; (4) Allen, 1963; (5) Cederblad 1946; (6) This paper, Table 1; (7) Wilson, 1953.

1967ApJ...147..490M

Table 6

DISTANCES AND RADIAL VELOCITIES OF OPTICALLY IDENTIFIED HII-REGIONS

1	2	3	4	5	6	7	8	9	10	11	
Source	N(NGC) I(IC)	$\alpha_{(1950)}$	$\delta_{(1950)}$	l^{II}	b^{II}	D kpc	v_r(heliocentric)/km sec^{-1}			+ −	$\lvert v_{ob} - v_{mod} \rvert$ km/sec^{-1}	
						Optical	Observed	Model AC	Model HK		AC	HK
OHP 109		00h 02.0m	+66° 40'	118.4°	+ 4.5°	---	-21.7 (2)					
G133.7+1.2	I 1795	02 21.7	+61 53	133.7	+ 1.2	2.42 (1)	-47.7 (6)	-43.3	-37.3	−	4.4	10.4
G133.8+1.4		02 22.8	+62 02	133.8	+ 1.4		-54.6 (6)			−	11.3	17.3
	I 1848	02 35.0	+61 15	135.4	+ 1.2	2.3 (1)	-32.8 (2)	-40.4	-35.5	+	7.6	2.5
	N 1499	04 02.0	+35 50	161.2	-12.1	0.3 (2)	+ 7.7 (2)	+ 3.7	- 1.0	+	4.0	8.7
	I 405	05 13.5	+34 25	172.0	- 2.1	0.6 (2)	+19.3 (2)	+ 5.8	+ 1.0	+	13.5	18.3
	I 410	05 20.0	+33 25	173.6	- 1.6	2.0 (1)	+ 8.2 (2)	+ 2.1	- 1.8	+	6.1	10.0
Orion A	N 1976	05 32.7	-05 25	209.0	-19.4	0.53 (1)	+16.1 (6)	+24.1	+16.4	+	8.0	0.3
λ Orion		05 36.0	+09 40	195.7	-11.4	0.6 (2)	+31.2 (2)	+19.8	+12.7	−	11.4	18.5
	I 434	05 39.0	-01 54	206.5	-16.4	0.4 (2)	+21.9 (6)	+21.9	+14.5	−	0.0	7.4
Orion Loop		05 42.5	+02 04	203.3	-13.7	0.4 (2)	+22.0 (2)	+21.0	+13.7	−	1.0	8.3
Ros. Neb.	N 2237	06 30.0	-05 00	215.3	- 6.5	1.4 (4)	+36.2 (2)	+38.1	+27.4	+−	1.9	8.8
	N 2264	06 38.5	+09 50	203.1	+ 2.2	0.715 (1)	+39.2 (2)	+22.9	+15.4	−	16.3	23.8
η Car. Neb.	N 3372	10 43.1	-59 25	287.6	- 0.6	1.6 (4)	+ 6.0 (7)	+ 1.3	- 3.0	+	4.7	9.0
ζ Orion		16 34.4	-10 28	6.3	+23.6	0.35 (1)	(+ 4.0 (2))	-13.0	-13.5	(−	17.0	17.5)
G353.2+0.9	N 6375	17 21.7	-34 06	353.2	+ 0.9	1.0 (5)	- 9.7 (6)	-12.1	-13.2	+	2.4	3.5
G353.2+0.7		17 22.4	-34 18	353.2	+ 0.7	1.0 (5)	-14.4 (6)	-12.1	-13.2	−	2.3	1.2
M 20	N 6514	17 59.0	-23 00	7.0	- 0.2	1.3 (3)	+ 0.9 (2)	- 7.3	- 8.2	−	8.2	9.1
M 8	N 6523	18 00.6	-24 52	6.0	- 1.2	1.1 (1)	- 8.1 (6)	- 8.2	- 9.2	−	0.1	1.1
M 16	N 6611	18 16.1	-13 52	16.9	+ 0.8	1.7 (1)	+13.5 (6)	- 0.2	- 0.5	−	13.7	14.0
M 17	N 6618	18 17.6	-16 12	15.0	- 0.7	1.8 (4)	+ 3.8 (6)	- 0.3	- 0.6	−	4.1	4.4
	N 6823	19 41.0	+23 12	59.4	- 0.1	2.48 (1)	+19.8 (2)	+ 7.6	+ 7.0	−	12.2	12.8
OHP 33		19 45.5	+28 05	64.1	+ 1.5		+ 8.5 (2)					
	N 6871	20 02.7	+54 52	89.0	+12.4	1.55 (1)	+ 4.1 (2)	-19.4	-19.2	+	23.5	23.2
OHP 546		20 17.0	+46 00	82.7	+ 5.7		(- 2.0 (2))					
OHP 56		20 18.0	+39 00	77.0	+ 1.6		+22.1 (2)					
OHP 59		20 25.0	+42 00	80.2	+ 2.3		-17.4 (2)					
	I 1318	20 26.0	+39 50	78.6	+ 0.8		-12.2 (2)					
Cyg Loop	N 6960	20 43.6	+30 32	73.3	- 7.6	0.7 (4)	-18.0 (7)	-11.4	-12.6	+	6.6	5.4
N. Amer. N.	N 7000	20 58.0	+44 30	85.9	- 0.9	1.13 (1)	-13.9 (2)	-15.3	-16.1	+	1.4	2.2
	I 1396	21 37.0	+57 00	99.1	+ 3.6	0.8 (1)	-17.2 (2)	-18.6	-19.2	+	1.4	2.0
OHP 92		22 18.5	+56 00	103.0	- 0.7	3.6 (2)	-52.0 (2)	-52.3	-44.1	+−	0.3	7.9
	N 7380	22 44.7	+57 50	107.0	- 0.9	2.38 (1)	-47.7 (2)	-38.5	-34.7	−	9.2	13.0
S 11		22 57.3	+58 30	108.8	- 1.0		-53.8 (2)					
	N 7635	23 18.5	+60 45	112.2	+ 0.1	2.75 (1)	-54.6 (2)	-47.2	-40.9	−	7.4	13.7
OHP 106		23 59.0	+64 30	117.6	+ 2.4		-53.8 (2)					

negative sign of the velocity difference in column 11 and similarly for positive values. Table 7 gives the mean velocity and the rms velocity dispersion of all twenty-eight H II regions and of the nine H II regions only, whose radial velocities have been determined from radio observations. The small mean velocity deviation $\langle(v_{obs} - v_{mod})\rangle$ shows that there is obviously no systematic deviation between the models of galactic rotation and the optical distance scale within an average distance of about 1.5 kpc from the Sun. The rms velocity dispersion given in the fourth and

TABLE 7

PECULIAR MOTION OF H II REGIONS

NUMBER OF H II REGIONS USED	MEAN VELOCITY $\langle(v_{obs}-v_{mod})\rangle$ (km sec^{-1})		RMS VELOCITY $\langle(v_{obs}-v_{mod})^2\rangle_{rms}$(km sec^{-1})		RMS VELOCITY* $\langle(v_{obs}-v_{mod})^2\rangle_{rms}$(km sec^{-1})	
	AC	HK	AC	HK	AC	HK
28	−1 33	−3 71	9 32	11 43	..	..
9	−2 83	−5 78	6 75	7 33	6 31	6 93

* Corrected for observational errors

fifth columns of Table 7 still contains the random error of our determination of the radial velocity, which is 2.4 km/sec. After subtracting this value geometrically, we obtain the velocity dispersions given in the sixth and seventh columns. If the optical radial velocities are included, we find a somewhat higher velocity dispersion. This may be due to a larger uncertainty in the optically derived radial velocities of about 7.7 km/sec. In this statistical analysis it has been assumed that distances of the H II regions obtained by optical methods have a negligible error. This assumption is certainly not true, and the velocity dispersions given in the sixth and seventh columns of Table 7 should hence be considered as an upper limit.

REFERENCES

Akabane, K , and Kerr, F. J. 1965, *Australian J. Phys.*, **18**, 91.
Allen, C. W. 1963, *Astrophysical Quantities* (2d ed.; London: Athlone Press).
Altenhoff, W., Mezger, P. G., Wendker, H., and Westerhout, G. 1960, *Veröff. Univ. Sternwarte Bonn*, No. 59, p. 48.
Baade, W., Goos, F , Koch, P. P., and Minkowski, R. 1933, *Z f. Ap.*, **6**, 355
Becker, W , and Fenkart, R. 1963, *Z. f. Ap.*, **56**, 257.
Broten, N. W., Cooper, B F , Gardner, F. F., Minnett, H. C , Price, R. M., Tonking, F. G., and Yabsley, D. E 1965, *Australian J. Phys.*, **18**, 85.
Burbidge, G. R., Gould, R J , and Pottasch, S. R 1963, *Ap. J.*, **138**, 945.
Campbell, W W., and Moore, J. H. 1918, *Pub. Lick Obs.*, **13**, 77.
Cederblad, S 1946, *Medd. Lunds Astr. Obs. Pub.* (2d ser., No. 119).
Clark, B G 1965, *Ap. J.*, **142**, 1398.
Courtès, G 1960, *Ann. d'ap* , **23**, 115.
Goldberg, L 1965, Discussion remark at the AAS meeting, Berkeley, Calif , December.
——— 1966, *Ap J.*, **144**, 1225.
Griem, H. R. 1967, *Ap. J.* (in press).
Hjellming, R M. 1966, *Ap. J.*, **143**, 420.
Höglund, B , and Mezger, P. G. 1965, *Science*, **150**, 339.
Hoerner, S von 1951, *Z. f. Ap.*, **30**, 17.
Hollinger, J P 1965, *Ap J.*, **142**, 609.
Howard, W. E , III, and Kirk, J. G. 1965, *A J.*, **70**, 434.
International Astronomical Union. 1963, *IAU Information Bull. No. 11.*
Kaler, J. B , Aller, L. H , and Bowen, I. S. 1965, *Ap. J.*, **141**, 912.
Kardashev, N. S 1959, *A.J.*, **36**, 838 (English trans., *Sov. Astr.—A.J.*, **3**, 813 [1960]).
Kerr, F. J , and Westerhout, G. 1965, *Stars and Stellar Systems*, ed. A. Blaauw and M. Schmidt (Chicago: University of Chicago Press), **5**, 167.
Kwee, K. K., Muller, C. A., and Westerhout, G. 1954, *B.A.N.*, **12**, 211.
Lilley, A. E., Menzel, D. H., Penfield, H., and Zuckerman, B. 1966, *Nature*, **209**, 468.

McGee, R. X., Robinson, B. J., Gardner, F. F., and Bolton, J. G. 1965, *Nature*, **208**, 1193.
Maxwell, A., and Downes, D. 1964, *Nature*, **204**, 865.
Menon, T. K 1961, *Pub. NRAO*, Vol. **1**, No. 1.
Mezger, P. G., and Henderson, A. P 1967, *Ap. J* , **147**, 471 (Paper I)
Mills, B. Y., Little, A. G., and Sheridan, K. V. 1956, *Nature*, **177**, 178.
Minkowski, R. 1934, *Z. f. Ap.*, **9**, 202.
Osterbrock, D. E. 1965, *Ap. J.*, **142**, 1423.
Palmer, P , and Zuckerman, B 1966, *Nature*, **209**, 1118.
Pottasch, S. R. 1965, *Vistas in Astronomy*, ed. A. Beer (London: Pergamon Press), **6**, 149.
Rougoor, G. W., and Oort, J. H. 1960, *Proc Nat Acad Sci.*, **46**, 1
Seaton, M. J. 1964, *M N* , **127**, 177.
Terzian, Y. 1965, *Ap. J.*, **142**, 135
Weaver, H , Dieter, N. H., and Williams, D. R. W. 1966, "OH in the Interstellar Medium: I. Emission in the Vicinity of H II Regions" (in preparation).
Weaver, H., Williams, D. R. W., Dieter, N. H., and Lum, W. T. 1965, *Nature*, **208**, 29.
Wilson, R. E. 1953, *Catalogue of Radial Velocities* (Carnegie Inst. of Washington Pub. 601).
Wilson, O. C , Münch, G , Flather, E , and Coffeen, M. 1959, *Ap. J. Suppl* , **4**, 199 (No. 40).
Zuckerman, B. 1966, paper presented at the URSI Spring meeting, Washington, D.C., April, 1966.